CHALMERS
UNIVERSITY OF TECHNOLOGY

Influence of alkali metals on combustion chemistry

The effect of sulfur additions and alkali metals interaction with the radical pool on CO oxidation in biomass combustion

Master's thesis in Sustainable Energy Systems

Oscar Gründer

Department of Energy and Environment
CHALMERS UNIVERSITY OF TECHNOLOGY
Gothenburg, Sweden 2016

Master's thesis 2016:ENMX04

Influence of alkali metals on combustion chemistry

The effect of sulfur additions and alkali metals interaction with the radical pool on CO oxidation in biomass combustion

Oscar Gründer

CHALMERS
UNIVERSITY OF TECHNOLOGY

Department of Energy and Environment
Division of Energy Technology
Chalmers University of Technology
Gothenburg, Sweden 2016

Influence of alkali metals on combustion chemistry
The effect of sulfur additions and alkali metals interaction with the radical pool on CO oxidation in biomass combustion
Oscar Gründer

© Oscar Gründer, 2016.

Supervisor: Fredrik Normann, Department of Energy and Environment
Examiner: Martin Seemann, Department of Energy and Environment

Master's Thesis 2016:ENMX04
Department of Energy and Environment
Division of Energy Technology
Chalmers University of Technology
SE-412 96 Gothenburg
Telephone +46 31 772 1000

Typeset in LaTeX
Gothenburg, Sweden 2016

Influence of alkali metals on combustion chemistry
The effect of sulfur additions and alkali metals interaction with the radical pool on CO oxidation in biomass combustion
Oscar Gründer
Department of Energy and Environment
Chalmers University of Technology

Abstract

This project investigates how alkali metals, chlorine and sulfur interact and affect the oxidation of CO and H_2 under post flame conditions. The investigation includes a test with sulfur additions in a 10 MW circulating fluidized bed(CFB) boiler and detailed reaction modelling of the combustion chemistry during conditions representative of the cyclone in the CFB boiler used in the experiments.

The experiments were performed by continuous and batch feeding of sulfur into the CFB boiler during operation with biomass. Temperatures and gas compositions in the boiler was measured. The other main method in this project was to model the combustion chemistry in the CFB boiler and its influence of K-S-Cl interactions. The detailed reaction modeling focused on how the combustion chemistry was affected by different K/S/Cl ratios by investigating reactions connecting the influence of K-S-Cl to oxidation of CO.

The results shows that the S/K ratio is important to the oxidation of CO. When sulfur was added in the experiments, CO concentration decreased drastically. Equilibrium calculations showed that K_2SO_4 is likely to form under present conditions. The modelling shows that sulfur additions decreases KOH content and forms K_2SO_4. KOH in excess of sulfur inhibits CO oxidation as it interacts with radicals important to CO oxidation. Excess KOH forms KO, which favours CO oxidation. Chlorine is most likely present as KCl and does not affect CO oxidation if KOH is in excess. The modelling does, however, not predict the significant decreases in CO oxidation during sulfur additions seen in the experiments. Continued work should focus on experimentally investigate the effect of the K/S ratios on CO oxidation under more controlled conditions in order to validate the models and develop the understanding of the mechanisms affecting CO oxidation.

Keywords: sulfur, alkali, combustion, radical, CO, potassium, chloride, Chemkin, biomass

Acknowledgements

I would like to thank my examiner Martin Seemann and supervisor Fredrik Normann for letting me do this thesis. The sessions where we have been discussing thesis related problems were always inspiring and fruitful as I came out with much more knowledge than before.

I would also like to thank Johannes Öhlin which helped me a lot in the early stage of the project when he guided me through the measurements that I got from the CFB boiler. Without him, it would not be possible to understand all the complex terminology used.

I would also like to thank the Ph.D students Thomas Ekvall and Teresa Berdugo Vilches for their kind help. Without their guidance and knowledge, my work would have taken much longer time and I would maybe not have recognized the conclusions that I now have drawn. A special thanks to Thomas, whose mechanism and thermodynamic files I have been used in Chemkin. I also would like to thank all the people at the Energy and Environment division for the pleasant environment at the office. The fika sessions have been great.

Finally, I would like to thank my parents Håkan Gründer and Agneta Gründer for their support during my whole life. During the project work they have also given me motivation at times when reaction mechanisms seemed too difficult to understand.

Oscar Gründer, Gothenburg, December 2016

Contents

List of Figures **xi**

List of Tables **xv**

1 Introduction **1**
1.1 Background . . . 1
1.2 Aim and scope . . . 4

2 Theory **7**
2.1 Combustion chemistry . . . 7
2.1.1 Radical pool reactions . . . 7
2.1.2 K/S/Cl reactions . . . 8
2.1.3 Volatile reactions . . . 11
2.1.4 Reactions between K/S/Cl and volatiles . . . 11
2.2 Chemical equilibrium . . . 12
2.3 Modelling theory . . . 12

3 Methods **15**
3.1 Evaluation of experiments . . . 15
3.1.1 Experimental setup and operation . . . 15
3.1.2 Evaluation methods . . . 17
3.2 Modelling of combustion chemistry . . . 18
3.2.1 General conditions and modelling tools . . . 18
3.2.2 Modelling procedure . . . 19
3.3 Comparison between experiment and modelling . . . 22

4 Results **23**
4.1 Evaluation of experiments . . . 23
4.1.1 Influence of continuous sulfur feeding . . . 23
4.1.2 Influence of batchwise sulfur addition . . . 28
4.2 Modelling of combustion chemistry . . . 30
4.2.1 Chemical equilibrium calculations . . . 31
4.2.2 Influence of sulfur and potassium . . . 32
4.2.3 Residence time and temperature dependency . . . 41
4.2.4 Influence of chlorine . . . 43
4.3 Comparison between experiment and modelling . . . 46
4.3.1 Parameter collection for the modelling . . . 46

4.3.2 Equilibrium calculation of experimental fractions 47
4.3.3 Model representation of the experiments 48

5 Conclusion **51**

6 Future work **53**
6.1 Setup of experiments 53
6.2 Experiments 53

Bibliography **55**

A Appendix 1 **I**
A.1 Integrated reactions rates I
A.1.1 The study varying SO_2 in section 4.2.2 I
A.1.2 Reactions path for KCl to K_2SO_4 III
A.1.3 Reactions of only sulfur III
A.2 Additional models IV
A.2.1 Residence time and temperature plots IV
A.2.2 Influence of more KCl than KOH VI
A.2.3 Sulfur equilibrium without K and Cl VII
A.3 Heat balance in the CFB boiler VIII

List of Figures

1.1 An overall presentation of the path of metals in biomass combustion in general. Different types of biomass have different amounts of the mentioned species. The darker mechanisms are focused in this project. 3

1.2 A simplified representation of the relationship between K, S, Cl, the radical pool and volatiles. Sulfur, potassium and chlorine affects the radical pool which affects the volatiles. 3

2.1 3 different paths for formation of K_2SO_4 from KCl and KOH during combustion with sulfur present. Side products are not shown and the species H and OH are present as radicals. 10

3.1 The CFB boiler that has been used for experiments. The positions where data have been collected are shown in the figure. The measurements for the gas analysis(specie concentration in the gas) are collected at H12, which is a probe that can measure at 9 different locations at the same height in the combustion chamber. This picture is not exactly showing the setup of the combustion chamber, but is only representing the features that are important in this project. . . . 16

4.1 CO concentration in ppm in the chimney vs time in minutes. Sulfur feeding was started at time 0. 23

4.2 CO concentration(%) in H12 positions before and after the start of sulfur feeding. R=Right, C=central, L=left side in the chamber. . . . 24

4.3 SO_2 and CO concentration in ppm in the chimney vs time where 0 is the time when sulfur injection was started. The blue is CO and the red is SO_2. 25

4.4 Temperatures(°C) in the combustion chamber for the top and bottom of the bed vs time in minutes. Time 0 is when the sulfur injection started. 26

4.5 Temperatures(°C) after the cyclone for 4 different measurements vs time in minutes. Time 0 is when the sulfur feeding was started. . . . 27

4.6 Concentrations(%) for species in H12. Upper left is O_2, upper right is CO_2, lower left is SO_2 and lower right is CO. F=Front(where the fuel is injected), C=centrum, B=Back, R=Right and L=Left 29

4.7 CO and SO_2 concentration(ppm) vs time in minutes during the occasions when sulfur was added. The x-axis is related to when sulfur was added. 30

4.8 Equilibrium fractions for KCl, KOH and K_2SO_4 vs temperature with 200 ppm K at the inlet. The plot is adjusted for K_2SO_4 so that each mole of K_2SO_4 is shown as 2 moles since it hold two moles of K. Blue is K_2SO_4, red is KCl and grey is KOH. 31
4.9 Equilibrium fractions for KCl and HCl vs temperature with 200 ppm Cl at the inlet. Blue is KCl and red is HCl. 32
4.10 CO outlet concentration vs inlet concentration of KOH in the first plot and the difference of inlet KOH minus 2*inlet of SO_2 in the second plot. The plots are representing SO_2 inlet concentrations where blue is 0ppm, red is 20, grey is 40 and yellow is 60 ppm. 33
4.11 Presentation of regions for different 2S/K ratios. The graph shows CO outlet concentration vs inlet concentration of KOH(Decreasing 2S/K ratio). SO_2 was kept constant at 40 ppm and no Cl species were included. The x-axis in this plot is not increasing linearly. 34
4.12 Fraction of species vs distance in the reactor. Blue is K, red is KOH, grey is K_2SO_4 and yellow is OH. All plots are from the case with 40 ppm SO_2 at the inlet. The upper left plot is for KOH inlet at 50 ppm, upper right at 90 ppm, lower left at 170 ppm and lower right at 250 ppm. This represents 2S/K fractions of 1.6, 0.89, 0.47 and 0.32 respectively. 35
4.13 Visualisation of the main reaction mechanism forming K_2SO_4 from KOH. Yellow means sulfur involvement, black means potassium involvement and blur means O/H involvement. i) is reaction 2.13, ii) 2.23, iii) 2.24, iv) 2.25 and v) 2.26. 36
4.14 CO outlet fraction vs inlet quota of 2 SO_2 per inlet fraction of KOH. Inlet fraction of KOH set to 300 ppm and temperature constant at 790 °C. 37
4.15 CO concentration(ppm) vs residence time(s) for different SO_2 inlets at different residence times. Blue shows 85 ppm SO_2 inlet representing region III(2S/K of 0.57), red 105 ppm SO_2 representing the optimum(2S/K of 0.7) and grey shows 125 ppm SO_2 representing region II(2S/K of 0.83). Temperature at 790 °C and KOH at 300 ppm. . . . 38
4.16 Reactions affected by KOH excess affecting CO oxidation. Black reactions includes potassium, yellow reactions includes carbon and blue reactions only includes O/H species. The arrows indicates if the specie is produced or consumed in the reaction. a) is Reaction 2.31, b) is 2.28, c) is 2.29, d) is 2.16, e) is 2.13, f) is 2.14, g) is 2.6, h) is 2.7, i) is 2.3 and j) is 2.8. 39
4.17 CO outlet vs 2S/K fraction. Blue has temperature 810 °C, red 830 °C and grey 850 °C. 42
4.18 Reaction rates(Mmol/cm^3s) vs residence time at 810, 830 and 850 °C in the early stage of the reactor. i) is reaction 2.28a, ii) is 2.28b, iii) is 2.31, iv) is 2.30 and v) is 2.32. 42
4.19 CO outlet(ppm) vs SO_2 inlet(ppm) for different inlet fractions of KCl. Blue has 0 ppm KCl, red 50, grey 100 and yellow 150. Inlet KOH kept constant at 300 ppm and temperature at 790 °C. 43

4.20 CO outlet(ppm) vs SO_2 inlet(ppm) for different inlet fractions of KOH and KCl. KOH concentration for blue is 150 ppm, red 200 ppm, grey 250 ppm and yellow 300 ppm. The left figure includes no KCl and the right figure includes KCl so the total amount of K is 300 ppm. . . 45
4.21 CO outlet vs SO_2 inlet for different inlet fractions of HCl. HCl concentration for blue is 0 ppm, red 50 ppm, grey 100 ppm and yellow 150 ppm. 45
4.22 KOH outlet vs SO_2 inlet for different inlet fractions of HCl. HCl concentration for blue is 0ppm, red 50ppm, grey 100ppm and yellow 150ppm. KOH inlet was always 300ppm. 46
4.23 Equilibrium fractions for KCl, KOH and K_2SO_4 vs temperature for the cases with and without sulfur feeding. The plot is adjusted for K_2SO_4 so that each mole of K_2SO_4 is shown as 2 moles since it hold two K molecules. Blue is KOH, red is KCl and grey is K_2SO_4. The inlet fraction of Cl is 8.4ppm, S is both 8.9 and 34ppm while K is 67 ppm. 48
4.24 CO concentration at the outlet of the PFR reactor vs inlet concentration of KOH. The blue plot represents the case without sulfur addition(SO_{2in} = 8.9ppm) and the red with the sulfur feeding(SO_{2in} = 34ppm). Temperature kept constant at 800° 49

A.1 Reaction path for S to SO_2. This model had 100ppm of S as inlet, no chlorine and no potassium. Reaction 1) is Reaction A.3, 2a) is A.4 and 2b) is A.5. III
A.2 CO outlet concentration vs 2S/K inlets for different residence times compared to the main residence time of 0.64s used. IV
A.3 CO outlet concentration vs 2S/K inlets for different residence times compared to the main residence time of 0.64s used. V
A.4 CO outlet concentration vs 2S/K inlets for different temperatures. . V
A.5 CO outlet concentration vs 2S/K inlets for different temperatures. . VI
A.6 CO outlet concentration vs 2S/K inlets for different amounts of KCl and KOH, where total K content is 300ppm. VII
A.7 Equilibrium calculation of sulfur species. S was added with 100ppm to the main flow without K or Cl species. VII

List of Tables

1.1 Properties of different fuels [4]. The values are shown in % and the proximate and ultimate analysis shows as dry fuel and the composition of ash as % of total ash. The first 5 fuels are biomasses whereas RDF(refuse-derived-fuels) have a significant amount of biomass but also other components. The data of wood chips are taken from analyses of the fuel in the Chalmers CFB boiler. Coal is shown as comparison. 2

3.1 Table of K-Cl-S species and temperatures in the different equilibrium models. Specie fractions are presented in ppm and temperatures in °. Equi 3 is shown in the section comparing the experiments with the modelling. 20

3.2 Table of K-S-Cl species, temperatures and residence time at the inlet of the different models. The specie fractions are shown as ppm. K/S represents the models where only K and S was varied. τ,T represents the models where residence time and temperature was varied. Cl represents the models where the influence of chlorine was studied. . . 21

4.1 Table of detected SO_2 due to the sulfur feeding. The mass of SO_2 is then translated into mass of sulfur, which eventually can be used to calculate the amount of sulfur that was detected as SO_2 compared to the amount of sulfur that was inserted. 25

4.2 Table of SO_2 in H12 and conversion of S from the inlets to SO_2 in H12. 26

4.3 Table of carbon species in different positions in the boiler. The conversion shows how much of the carbon from the fuel that is present as CO and CO_2 in H12. The CO and CO_2 was measured in H12 and outlet before and after sulfur feeding. 28

4.4 Table of detected SO_2 after sulfur additions. The mass of SO_2 is then translated into corresponding mass of sulfur, which was used to calculate the fraction of injected sulfur detected as SO_2 in the chimney. 30

4.5 Table of integrated reaction rates(kmol/m^3) for the cases with different inlet fractions of SO_2 39

4.6 Table of the specie molar fractions kept constant as inlets of the PFR in the modelling. 47

4.7 Table of S, Cl and K molar fractions calculated from experiments that was used in the modelling. 47

A.1 Table of integrated reaction rates(kmol/m^3) including KOH for the cases with different 2S/K ratios. I
A.2 Table of integrated reaction rates(kmol/m^3) including KOH for the cases with different 2S/K ratios. II
A.3 Table of integrated reaction rates(kmol/m^3) including KOH for the cases with different 2S/K ratios. II
A.4 Table of integrated reaction rates(kmol/m^3) including OH reaction for the cases with different 2S/K ratios. II
A.5 Table of integrated reaction rates(kmol/m^3) including OH reaction for the cases with different 2S/K ratios. III

1
Introduction

In this project studies are made on how sulfur, chlorine and alkali metals affect the combustion chemistry. The topic had been increasing in interest and when a study on sulfur additions in a circulating fluidized bed boiler yielded full oxidation of CO, there was a good motivation to start this project. In this section, a background broadly describing biomass in combustion and alkali metals interaction with sulfur is presented, as well as the aim and scope.

1.1 Background

Biomass used for heat and power production is not considered as a fossil fuel since it grows fast and capture CO_2 from the air during its growth[1]. According to the International Energy Agency(IEA) the world used about 66.7% of fossil fuel for electricity in 2014[2]. The combustion of biomass to produce heat and power becomes more popular for every day since countries have to reduce their use of fossil fuels. There is a great interest to investigate the phenomenas during combustion of biomass thoroughly, since the use will most probably be extended in the future. It will also help the argument for countries to invest in biomass combustion processes if the problematic issues are solved.

A growing rate of biomass combustion has led to that different types of biomass are used as fuel. They have slightly different compositions but have similar amounts of the same species. Trees are mainly constituted of water, cellulose, hemicellulose and lignin and the main atoms in biomass are therefore C, H and O. However, there are also other types of atoms present such as metals from ashes, N, Cl and S but to a lesser extent. These latter components may vary more for different types of biomass but the property that biomass have in common is that they have more alkali metals and much less sulfur than other types of fuel, such as coal and peat, see Table 1.1. Table 1.1 shows that straws contain much more chlorine than other biomass and that coal has significantly more sulfur and less potassium than biomass. These properties of biomass leads to serious corrosion issues on walls and on heat exchanger materials at high temperatures inside the combustion chamber[3]. Further in this project, only wood chips is considered however.

Table 1.1: Properties of different fuels [4]. The values are shown in % and the proximate and ultimate analysis shows as dry fuel and the composition of ash as % of total ash. The first 5 fuels are biomasses whereas RDF(refuse-derived-fuels) have a significant amount of biomass but also other components. The data of wood chips are taken from analyses of the fuel in the Chalmers CFB boiler. Coal is shown as comparison.

Specie	**Wheat straw**	**Willow wood**	**Mixed paper**	**Fir mill**	**Wood chips**	**RDF**	**Coal**
Proximate analysis							
Fixed carbon	17.71	16.07	7.42	17.48	19.71	0.47	77.00
Volatile matter	75.27	82.22	85.25	82.11	79.82	73.40	18.49
Ash	**7.02**	**1.71**	**8.33**	**0.41**	**0.49**	**26.13**	**4.51**
Ultimate analysis							
C	44.92	49.9	47.99	51.23	50.4	39.70	87.52
H	5.46	5.90	6.63	5.98	6.13	5.78	4.26
O	41.77	41.8	36.84	42.1	42.79	27.24	1.55
N	0.44	0.61	0.14	0.06	0.11	0.80	1.25
S	**0.16**	**0.07**	**0.07**	**0.03**	**0.02**	**0.35**	**0.75**
Cl	**0.23**	**0.01**	**0**	**0.19**	**0.01**	**0**	**0.16**
Ash	7.02	1.71	8.33	0.41	0.49	26.13	4.51
Composition of ash							
SiO_2	55.32	2.35	28.10	15.17	4.11	33.81	37.24
Al_2O_3	1.88	1.41	52.56	3.96	0.83	12.71	23.73
TiO_2	0.08	0.05	4.29	0.27	0.09	1.66	1.12
Fe_2O_3	0.73	0.73	0.81	6.58	0.68	5.47	16.83
CaO	6.14	41.2	7.49	11.90	32.55	23.44	7.53
MgO	1.06	2.47	2.36	4.59	5.99	5.64	2.36
Na_2O	1.71	0.94	0.53	23.50	0.83	1.19	0.81
K_2O	**25.6**	**15.0**	**0.16**	**7.00**	**18.19**	**0.20**	**1.81**
SO_3	4.4	1.83	1.7	2.93	-	2.63	6.67
P_2O_5	1.26	7.4	0.2	2.87	3.53	0.67	0.10
CO_2/other		18.24		18.92	?		
Undetermined	1.82	8.38	1.8	2.31	?	12.58	1.80

Figure 1.1 show a presentation of how metals are released and further reacted in the combustion chamber. As the metals are released they are rapidly oxidized, chlorinated or sulfated. From there it can undergo different operations such as condensation or corrosion depending on the conditions in the combustion chamber. However, this project only focuses on the gas phase chemistry, excluding the heterogeneous effects, ash formations, corrosion and agglomeration which also is present in combustion.

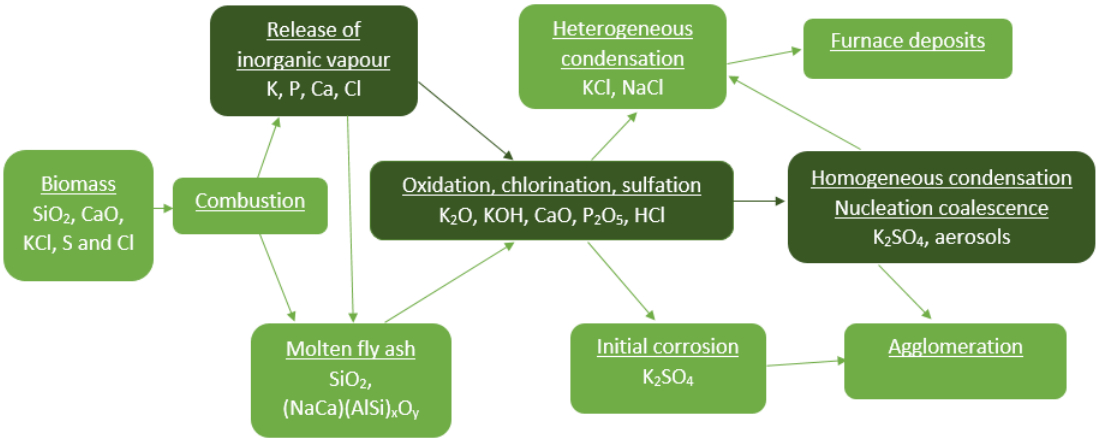

Figure 1.1: An overall presentation of the path of metals in biomass combustion in general. Different types of biomass have different amounts of the mentioned species. The darker mechanisms are focused in this project.

One way to decrease the corrosion is to reduce the temperature, but that leads to significant lower efficiency. Therefore studies have been made finding reactions decreasing the corrosive substances, such as KCl, in the flue gas. Via reactions with radical species such as O, H and OH radicals and sulfur, K_2SO_4 is formed [5]. This is an aerosol which creates a layer at the heat exchanger equipment just as KCl, but is much less corrosive and therefore concerned as a wanted product in comparison to KCl. The formation around the heat exchangers are made by condensation via heterogeneous nucleation[6]. These studies have proven that the set of K-S-Cl interacts with the radical pool and since it is known that the volatiles H_2/CO interacts with the radical pool to oxidize, it is suggested that K-S-Cl affects the volatiles via the radical pool. Figure 1.2 shows an overall simple relationship between the species. Potassium may affect the radical pool by itself or together with chlorine and sulfur. It has though not yet been investigated whether K/S/Cl affects volatiles directly but was investigated in this project.

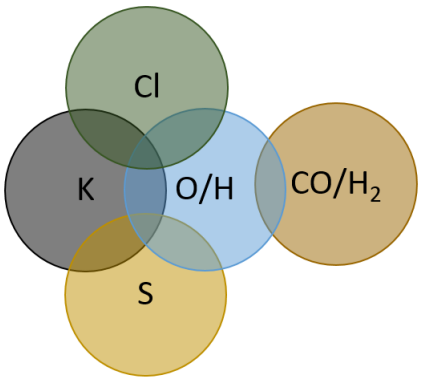

Figure 1.2: A simplified representation of the relationship between K, S, Cl, the radical pool and volatiles. Sulfur, potassium and chlorine affects the radical pool which affects the volatiles.

It has been shown that there are different reaction paths for the transformation

of the alkali metals from KCl to K_2SO_4 [5]. Since there are very low contents of sulfur in biomass, the sulfur has to be added in some way in order to reduce the KCl concentration. Different additives can be added in order to decrease KCl, for example aluminum silicate, sulfur or calcium based additives[7]. One promising reaction path is to add SO_3 by ammonium sulfate, $(NH_4)_2SO_4$, that along with O_2 sulphates KCl into K_2SO_4[8]. It has also been shown that injecting elementary sulfur, which oxidizes into SO_2, can sulfate KCl into K_2SO_4, but that reaction path has shown to not be as efficient as the path with SO_3. Other studies have investigated how the ammonium sulfate injection should be made for best efficiency. It has shown that even a small presence of combustibles as well as low oxygen presence decreases that sulfation of KCl [9]. Some experiments have shown that co-combustion of biomass together with a sulfur containing material can be effective to sulfate KCl. It has been done with peat, coal and sewage sludge and has shown promising results in KCl reduction[10]. K_2CO_3 is also a molecule that may be likely to form from released potassium in biomass combustion.

Recent experiments have shown that different amounts of potassium affects CO burnout, which leads to further questions on how and why this small fraction of alkali metals affect the whole combustion process. Since CO undergoes oxidation after the hydrocarbons, it can be present when sulfur is injected. CO is also slower than H_2 to oxidize so CO is more likely to be affected when the mechanisms in the radical pool is changed. CO needs the O/H radicals in order to be fully oxidized into CO_2, but the sulfation mechanisms of KCl into K_2SO_4 also uses those radicals[8]. If the radical pool interacts with the sulfation process of potassium it means that less potassium is present during the CO oxidation. Since previously made experiments indicated that sulfur additions improved CO oxidation it was suggested that potassium hinders CO oxidation. Studies with the oxyfuel process(using oxygen a higher share of oxygen than with air) has, in contrast, shown that the presence of potassium improves CO oxidation[3]. How these observations can be explained will be further investigated in this project.

Injecting sulfur may improve CO oxidation but if the injected sulfur does not form K_2SO_4 and condensate, it will mainly be present as SO_2 in the exhaust gas. SO_2 is concerned as an environmental unfriendly gas since it acidifies the ground nearby. There are hard restrictions on SO_2 emissions for power plants, that implies that if sulfur should be added, all sulfur has to react into species that is not acidifying the surroundings.

1.2 Aim and scope

Previous studies investigating formation of K_2SO_4 have not put focus on its effects on the main combustion chemistry of volatiles. This project will instead study how alkali metals and sulfur injections, creating different K/S/Cl ratios, affect the combustion chemistry, mainly in terms of CO oxidation. Since there are regulations on CO emissions and that full oxidation of CO means increased efficiency, these investigations can lead to suggestions on how to improve boilers in the future.

The objective is to identify and explain the influence of alkali metals in the combustion process in such way that the general understanding for the subject is improved. The project will try to map how the radical pool chemistry is affected by different K/S/Cl ratios, in terms of gas phase reactions. The mapping may lead to suggestions on which reaction mechanisms that are dominant and what are the favourable conditions for these mechanisms. The project will investigate how different types of sulfur additions in a CFB boiler affect the CO oxidation and also how dependent the kinetics from the sulfur additions are on residence time. Since most K-S-Cl species are not measured, it will be investigated how K, S and Cl are present by equilibrium calculations. Due to uncertainties and variations between boilers, operating conditions such as temperature, specie fractions and residence time should be varied to perform representative studies. When these broad studies have covered reasonable conditions, the project can suggest what operating conditions that are favourable in terms of CO oxidation and how unfavourable conditions can be improved.

2
Theory

In this section, the combustion chemistry including volatile, K/S/Cl and radical reactions will be explained. A brief explanation of chemical equilibrium and how the modelling operates are also presented. The heavy part of this project has been on the reactions and equations was not necessarily advanced.

2.1 Combustion chemistry

There is a large network of reactions taking place in the combustion process of biomass and there are many intermediate products before the biomass is oxidized into CO_2 and H_2O which is the main combustion products. The combustion chemistry is sometimes simplified to that biomass, which mainly consists of C, H, and O will together with O_2 eventually form only CO_2 and H_2O as described by as: $C_mH_nO_p + (m + \frac{n}{4} - \frac{p}{2})O_2 \longrightarrow mCO_2 + \frac{n}{2}H_2O$. Carbon oxidizes into multiple intermediate products but the main reactant to the last reaction into CO_2 is usually CO. However, due to equilibrium CO and H_2 is also present as products but only in small fractions. When biomass is oxidized energy from the chemical bonds and radiation is released.

As have been mentioned earlier, the radical pool of O/H species reacts both with the K/S/Cl group and with volatiles CO/H_2. This section do not cover all reactions, only the key reactions taking place. However, there are many reactions needed to mention since they are crucial in some cases.

2.1.1 Radical pool reactions

Hydrogen and oxygen is dissociating and forming radicals during combustion due to the high temperature. A radical is a molecule that has one unpaired electron which is very reactive and for example reacts with the volatiles in combustion. The reactions that takes place in the radical pool can be grouped into initiation, branching, propagation and termination reactions. In initiation reactions, two radicals are produced and where the reactants are no radicals. In chain branching one radical is consumed and two radicals formed. Propagation however is when one radical is formed and one is consumed and termination is when one or more radicals are consumed but no one is formed.

The initiation of the radical pool comes mainly from the Reaction in 2.1 and 2.2

and is then taken over by the other radical reactions. Chain branching reaction are shown in Reaction 2.3, 2.4, 2.5 and 2.6[11][12]. The radicals can then continue with propagation reactions such as Reaction 2.7 and termination within the radical pool such as Reaction 2.8. The radicals that are of greater importance are O, H, OH and HO_2 whereas species as H_2O, O_2 and H_2 are important by formation and consumption of radicals.

$$H_2 \longrightarrow 2\,H \tag{2.1}$$

$$O_2 \longrightarrow 2\,O \tag{2.2}$$

$$O_2 + H \longrightarrow OH + O \tag{2.3}$$

$$H + O_2 \longrightarrow HO_2 \tag{2.4}$$

$$H_2 + O \longrightarrow OH + H \tag{2.5}$$

$$O + H_2O \longrightarrow 2\,OH \tag{2.6}$$

$$HO_2 + H \longrightarrow 2\,OH \tag{2.7}$$

$$HO_2 + OH \longrightarrow H_2O + O_2 \tag{2.8}$$

2.1.2 K/S/Cl reactions

The K/S/Cl ratio in biomass differs a lot from coal in terms of less sulfur and more potassium. Since this project considers different ways to add sulfur, the reactions of sulfur are of great importance. Solid sulfur, which is added, oxidise quickly into SO_2 by O_2 in Reaction 2.9 or by OH in Reaction 2.10[13]. From there, the SO_2 can oxidise further into SO_3 as in 2.11 directly or via intermediate step 2.12. However the formation of SO_3 is not that likely to occur with the operating conditions used in this project.

$$S + OH \longrightarrow H + SO \tag{2.9a}$$

$$SO + OH \longrightarrow SO_2 + H \tag{2.9b}$$

$$S + O_2 \longrightarrow SO + O \tag{2.10a}$$

$$SO + O_2 \longrightarrow SO + O \tag{2.10b}$$

$$SO_2 + HO_2 \longrightarrow SO_3 + OH \tag{2.11}$$

$$SO_2 + OH \longrightarrow HOSO_2 \tag{2.12a}$$

$$HOSO_2 + O_2 \longrightarrow SO_3 + HO_2 \tag{2.12b}$$

The interaction of KOH with radicals are important since that may affect the overall combustion chemistry. KOH can interact with H and form K according to Reaction 2.13 and K can react back to KOH via reaction 2.14 and 2.15[6]. KO can also be formed with Reaction 2.16 and 2.18 whereas $K_2(OH)_2$ can be formed via Reaction 2.17[6].

$$KOH + H \longrightarrow K + H_2O \tag{2.13}$$

$$K + HO_2 \longrightarrow KOH + O \tag{2.14}$$

$$K + OH \longrightarrow KOH \tag{2.15}$$

$$KOH + OH \longrightarrow KO + H_2O \tag{2.16}$$

$$2\,KOH \longrightarrow K_2(OH)_2 \tag{2.17}$$

$$K + O \longrightarrow KO \tag{2.18}$$

The most important reactions with chlorine and potassium are Reaction 2.19, forming HCl and 2.20, forming KCl. Reaction 2.19 interacts with the radical pool by consuming a H radical. KCl, K and KOH can then be further reacted with sulfur.

$$H + KCl \longrightarrow HCl + K \tag{2.19}$$

$$KOH + HCl \longrightarrow KCl + H_2O \tag{2.20}$$

In Figure 2.1 the most common reaction mechanisms for KCl and KOH to K_2SO_4 are shown, but several studies suggests that the path with SO_3 are more important than the pathways with SO_2[6] [8]. However, SO_3 may be of greater importance in this project. When K_2SO_4 is formed, it will condensate and sit on the heat exchanger equipment in the boiler by heterogeneous nucleation. The reactions in Figure 2.1 are gas phase only. When K_2SO_4 is formed it can condensate on surfaces in the boiler.

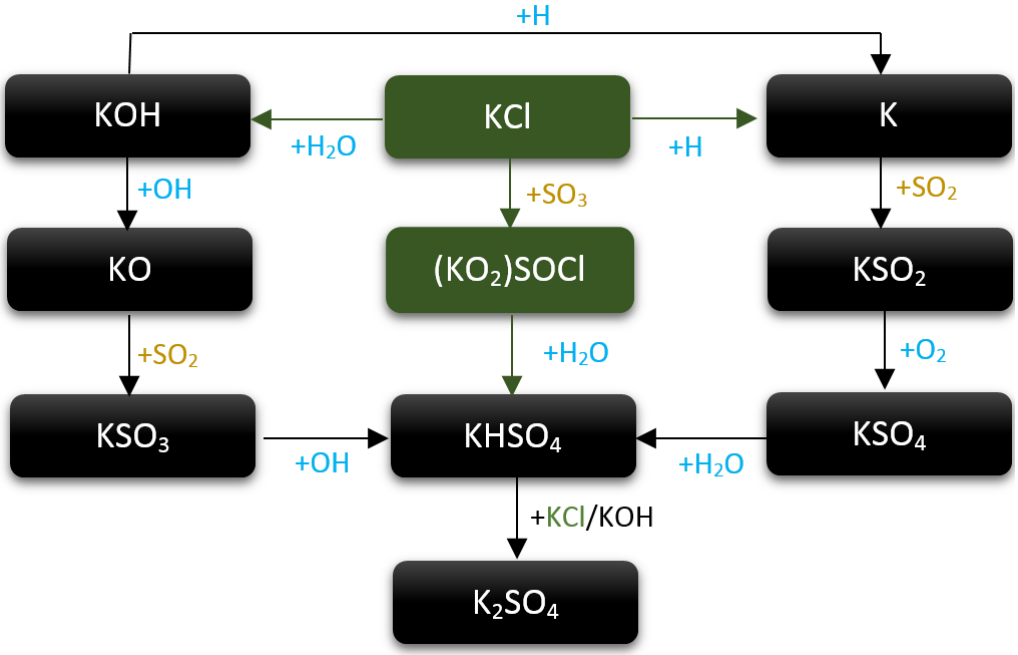

Figure 2.1: 3 different paths for formation of K_2SO_4 from KCl and KOH during combustion with sulfur present. Side products are not shown and the species H and OH are present as radicals.

The reaction mechanisms of the sulfation of KCl into K_2SO_4, which is visualised in Figure 2.1, are assembled in overall reactions shown in Reaction 2.21 where only KCl is considered as the starting molecule[8][3]. These reactions consumes sulfur and species from the radical pool, forming HCl together with K_2SO_4. The last reaction is interesting since it produces an OH radical and consumes a H radical, which may enhance CO oxidation.

$$2\,KCl + SO_2 + 2\,OH \longrightarrow K_2SO_4 + 2\,HCl \tag{2.21a}$$

$$2\,KCl + SO_3 + H_2O \longrightarrow K_2SO_4 + 2\,HCl \tag{2.21b}$$

$$2\,KCl + H + SO_2 + O_2 + H_2O \longrightarrow K_2SO_4 + 2\,HCl + OH \tag{2.21c}$$

However, when there are no chlorine it is likely that potassium is released as KOH and the assembled overall reaction mechanisms are presented in Reaction 2.22. Like in the case with KCl, the last mechanism produces one OH radical and consumes one H radical.

$$2\,KOH + SO_2 + 2\,OH \longrightarrow K_2SO_4 + 2\,H_2O \tag{2.22a}$$

$$2\,KOH + H + SO_2 + O_2 \longrightarrow K_2SO_4 + H_2O + OH \tag{2.22b}$$

As mentioned earlier, KOH and KCl can be reacted to K via Reactions 2.13 and 2.19, which then may form K_2SO_4 via the Reactions 2.23, 2.24, 2.25 and 2.26, also

seen as the reaction mechanism to the right in Figure 2.1[3]. Reaction 2.27 may also occur as a side reaction forming K_2SO_4 straight from KSO_4.

$$K + SO_2 \longrightarrow KSO_2 \tag{2.23}$$

$$KSO_2 + O_2 \longrightarrow KSO_4 \tag{2.24}$$

$$KSO_4 + H_2O \longrightarrow KHSO_4 + OH \tag{2.25}$$

$$KHSO_4 + KOH \longrightarrow K_2SO_4 + H_2O \tag{2.26}$$

$$KSO_4 + KOH \longrightarrow K_2SO_4 + OH \tag{2.27}$$

2.1.3 Volatile reactions

There are a large amount of volatiles in biomass, around 80 % compared with coal which only has around 18 % volatiles and much more fixed carbon. Volatiles are the species that vaporises when the fuel is heated in presence of air. The compounds that are volatile gets oxidised by the radical species and forms CO and H_2 before finally oxidise into CO_2 and H_2O. This last oxidation step takes place by Reaction 2.28 and 2.29, where also 2.30 occurs at a smaller extent[12]. Reaction 2.28 is the main reaction oxidising CO to CO_2, thus is very important in this project.

$$CO + OH \longrightarrow CO_2 + H \tag{2.28}$$

$$H_2 + OH \longrightarrow H_2O + H \tag{2.29}$$

$$CO + O \longrightarrow CO_2 \tag{2.30}$$

2.1.4 Reactions between K/S/Cl and volatiles

There are also reactions that occurs between the K/S/Cl group and the volatiles, meaning that the interaction between them does not necessarily have to go through the radical pool. The direct interaction of chlorine and sulfur with H_2 and CO are not of an significant magnitude in this project but two potassium reactions with CO are shown in Reactions 2.31 and 2.32, where Reaction 2.31 will have an important role in CO oxidation in this project.

$$KO + CO \longrightarrow K + CO_2 \tag{2.31}$$

$$KO_2 + CO \longrightarrow KO + CO_2 \tag{2.32}$$

2.2 Chemical equilibrium

Reactions are sometimes not complete due to chemical equilibrium occurs at a point where the concentrations of reactants and products do not change over time. That position is when the Gibbs free energy is at its minimum, which is described in Equation 2.33 at constant temperature and pressure. Both forward and backward reactions are taking place at the same rate when chemical equilibrium is reached. K_p is the equilibrium constant and can be described as in Equation 2.34 where A and B are reactants while R and S are products.

$$G = H - TS = RTln(K_p) \tag{2.33}$$

$$K_p = \frac{p_R^r p_S^s}{p_A^a p_B^b} = \frac{n_R^r n_S^s}{n_A^a n_B^b} \Big(\frac{p}{\sum n_i} \Big)^{r+s-a-b} \tag{2.34}$$

K_p for a reaction can also be expressed as in equation 2.35, where C_1 and C_2 is constants for each reaction.

$$K_p = C_1 * exp\big(\frac{C_2}{T}\big) \tag{2.35}$$

In this project, equilibrium for potassium, sulfur and chlorine species are investigated. The chlorine is mainly released as HCl and KCl in combustion of biomass. Chlorine is usually present in a less content to alkali metals in biomass meaning that only equilibrium is determining whether chlorine is present as HCl or KCl. HCl is an acid but KCl is corrosive making HCl the wanted product of the chlorine species. The potassium is present to a larger extent in biomass than in coal and there have been several problems with this specie concerning corrosion and fouling on energy equipment. The potassium is released as KOH or KCl and Equilibrium 2.36 presents an equilibrium reaction in which KCl and KOH concentration can vary. When the species are at equilibrium concentrations, the reactions between them will still occur, but in the same rate.

$$\mathrm{KOH + HCl \rightleftharpoons KCl + H_2O} \tag{2.36}$$

Sulfur, which is added in its elementary form will be rapidly vaporized when inserted to the boiler. The phase shift is not considered in this project but there will be a chemical equilibrium in gas phase between SO_2 and SO_3 depending on temperature. However, K_2SO_4 may also be present due to equilibrium, which will be investigated.

2.3 Modelling theory

The modelling program Chemkin imports thermodynamic data such as enthalpy, entropy and C_p values for all species as well as constants for the mechanisms modified Arrhenius expression. The modified Arrhenius expression is shown in Equation 2.37 where A is the pre-exponential factor, T is temperature, β is the temperature exponent, E_a is the activation energy and R is the gas constant. A, β and E_a are

taken from the data file for each reaction mechanism. When the reaction constant k is obtained, the model could calculate the concentration for the next cell downstream the reactor.

$$k = AT^{\beta}e^{\frac{-E_a}{RT}} \tag{2.37}$$

Chemkin gives reaction rates for all reactions in all positions of the reactor. By integrating these reaction rates over increasing residence time in the boiler, the amount of reactions can be calculated. The integration can be made by the trapezoidal method which is a numerical integration by discrete input data. In Matlab the function is called "trapz" and performs integration over multiple intervals by breaking the total area under the graph into smaller areas. The integration is performed as described in Equation 2.38.

$$\int_a^b f(x)dx = \frac{b-a}{2N}\sum_{n=1}^{N}(f(x_N) + f(x_{N+1}) \tag{2.38}$$

3
Methods

There have been two main methods to investigate the reaction properties of the alkali metals, which are data evaluation of a previously made experiment and modelling of the reaction mechanisms between K/S/Cl, radicals and volatiles. The evaluation of experiments and modelling were compared in order to see how well the resulting trends matched. All methods have used operating conditions such as biomass in the fuel, excess air ratio of 1.2 and the main focus in the overall combustion has been in the late part of combustion where only CO and H_2 are left to oxidise. The data evaluation investigated how the K/S/Cl set affects CO/H_2, not looking into detail at the intermediate step with the radical pool. The modelling did however investigate how the radical pool interacts with the K/S/Cl set and volatiles. At the end of the project new experiments were suggested for future work.

3.1 Evaluation of experiments

The experimental evaluation included experiments from two days where elementary sulfur was injected in different ways in a CFB boiler burning wood chips. Temperatures in different areas of the CFB boiler, gas compositions in the top of the combustion chamber, pressure drop over the boiler, weight of bed material and mass flows were collected for both days. That data was extracted and analyzed in this project. The analysis was made by plotting the data to identify trends and calculating mass balances and conversions of species.

3.1.1 Experimental setup and operation

The CFB boiler configuration is presented in Figure 3.1. Gas compositions were measured in the upper part of the furnace, called H12, and in the chimney where temperatures were measured in the whole system. The particle distributor can be used to attach the boiler to a gasifier, but this was however not used in these experiments and is thus not shown in the figure. These experiments have used a bed material of olivine sand which is a mix of mainly MgO, SiO_2 and Fe_2O_3[14]. Since the sand is a mix of different species, it has different melting point depending on the ratio between the species. The bed material flows between the combustion chamber and the cyclone.

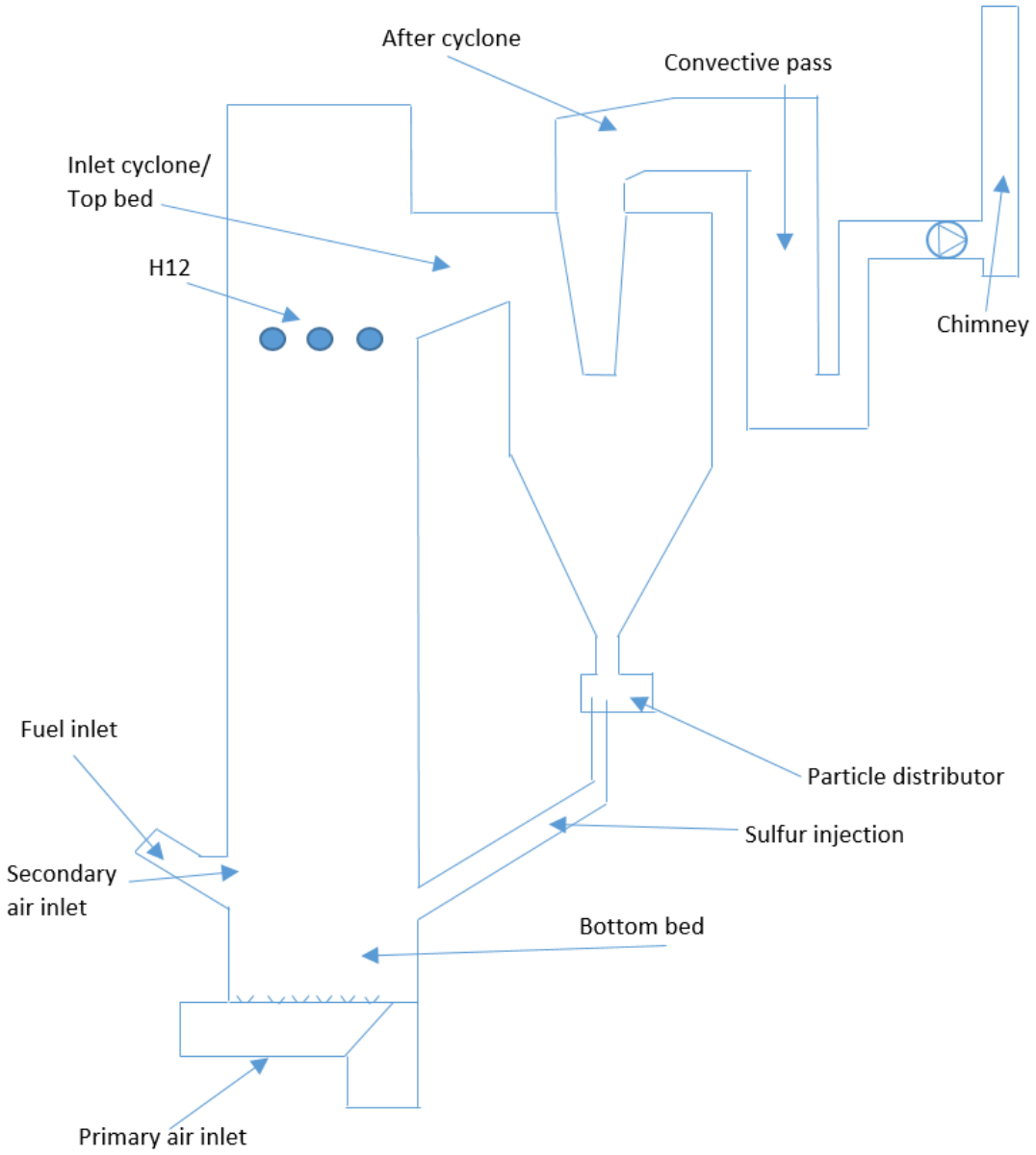

Figure 3.1: The CFB boiler that has been used for experiments. The positions where data have been collected are shown in the figure. The measurements for the gas analysis(specie concentration in the gas) are collected at H12, which is a probe that can measure at 9 different locations at the same height in the combustion chamber. This picture is not exactly showing the setup of the combustion chamber, but is only representing the features that are important in this project.

The devices measuring concentrations can only measure dry matter, so the water content is therefore not included in the measurements. By knowing the moisture content from a fuel analysis, the real concentrations could be calculated including the moisture content. The devices measure concentration in volume percentage and thus makes it necessary to use densities to convert the concentrations into mass flows and then use molar mass to convert into molar flows.

The experiments were performed to measure how two different injection methods of sulfur affected the combustion process. One experiment was made where sulfur was injected by a constant flow from the return pipe. Data was collected both before and after the constant feeding was started. In H12, measurements of gas compositions were taken only in the middle row.

Another experimental type was made where sulfur was added batchwise, four times at the top of the cyclone and two times in the return pipe. About two minutes after the fifth addition, a constant addition of sulfur granules in the return pipe was started. After the last addition the pressure in the chamber decreased rapidly and thus the results from there were not reliable. The first sulfur addition was made with approximately 30 g and the rest with 85 g of elementary sulfur. Measurements in all 9 positions in H12 were made between the third and the fourth measurement where no added sulfur was predicted to be present.

3.1.2 Evaluation methods

The measurements gave rather high fluctuations which made it necessary to use averaging to achieve representative numbers. Although averaging was made, still large uncertainties comes with these values. The devices may be poorly calibrated and due to high fluctuations and few measuring points were collected, it is adding uncertainty over the validness of the numbers. These plots and calculations should not be regarded as scientifically valid but are better to see as identifying trends and give rough estimations of the influence of the sulfur additions. The plotting has been made in Excel and the calculations in Matlab. Since not that advanced calculations were performed, it was not necessary to use more detailed and advanced software.

Calculations on specie fractions were made in order to understand to calculate conversion and to prepare parameters for the modelling and conversion calculations. The measured species in H12 and the chimney could be used to compare with the calculated specie fractions in order to validate the calculations. The total mass flow was calculated by summing the air flow and fuel flow. The inlet specie fractions were calculated by importing data from a fuel analysis which contained an ultimate analysis and ash analysis giving information of how large fraction of each atom that was present. The fractions of the air was assumed to be 79% N_2 and 21% O_2 and the inlet mass flow for each specie could be calculated. Only potassium was considered of the metals.

The outlet fractions could then be calculated by using convenient assumptions. It was assumed that all carbon were present as CO or CO_2 at the outlet. N_2 was assumed to be inert and 2/3 of the fuel N was assumed to be present as N_2, the rest as NO. All chlorine was assumed to be present as KCl and the remaining potassium to be present as KOH. The sulfur was assumed to be present as SO_2 and the missing concentration from the measurement could be assumed to be due to formation of K_2SO_4. Equilibrium calculations between H_2O and H_2 were made using Equation 2.34 importing data from the reaction $H_2O \rightleftharpoons H_2 + \frac{1}{2} O_2$ which was chosen as the

equilibrium reaction between H_2 and H_2O. Alas, the O_2 concentration was still not known leading to that concentrations for CO and CO_2 was used and implemented by the equilibrium reaction of $CO + \frac{1}{2} O_2 \rightleftharpoons CO_2$. However, the measuring probe for the gas compositions in the boiler can not measure wet content, meaning that H_2O is excluded. The steam content had to be taken into account calculating total mass flow in order to compensate for the missing measurement from the probe. The measurements were made in H12 and chimney, which were imported by averaging the measurements.

The obtained specie fractions was used to calculate the conversions in the boiler. The calculated inflow of sulfur, both from the fuel and from the injection, was used to compare with the measured outlet fraction of SO_2. Equation 3.1 shows how the detected mass of SO_2 in the chimney was calculated by the measured SO_2 fraction(x_{SO_2}) in the chimney . The sulfur injections were used as tracer experiments where the outlet concentration verses time was plotted and its integral gave the amount of SO_2 that was detected per sulfur injection. The amount of sulfur injected was compared with the amount of SO_2 in the outlet, giving a conversion rate(X_{SO_2}), as seen in Equation 3.1 and 3.2. Three sulfur injections, number 2, 3 and 4, were used for the calculations where 85 g of sulfur was injected in each addition. The other injections gave a too small detection in the chimney to be able to perform reliable calculations.

$$m_{SO_2 detected} = m_{tot} \int_{t_1}^{t_2} x_{SO_2}(t)dt \tag{3.1}$$

$$X_{SO_2} = \frac{n_{SO_2 detected}}{n_{Sinserted}} \tag{3.2}$$

3.2 Modelling of combustion chemistry

Modelling was made in order to understand the reaction mechanisms between the K/S/Cl species, radical pool and volatile species. The modelling has focused on reaction mechanisms during the later part of the combustion and on how various K/S/Cl fractions affect the combustion chemistry, mainly CO oxidation.

3.2.1 General conditions and modelling tools

The program used for the modelling was Chemkin. Chemkin was used since it is a fast modelling program that uses simple reduced reaction mechanisms for kinetic simulations. In order to keep modelling simple and to have a larger focus on the kinetics, a plug flow reactor(PFR) was used as reaction domain. It has been chosen to perform the modelling with a fixed gas temperature and not solve the energy equation since the reactions that take place does not affect the temperature significantly. The same dimensions and flows as the part of the boiler after the cyclone have been chosen as the reactor dimensions in order to create a similar environment. Being more precise, specie fractions from H12, mass flows and temperatures were imported from the CFB boiler. The model performed the procedure of the part

after H12 and investigated how sulfur injections affect certain reaction mechanisms. Using PFR and importing specie fractions from H12 may be incorrect since the cyclone is stirring the flow and most probably more reactions takes place there. The reaction mechanism set was used from a previous study of K-S-Cl species during combustion of propane. The mechanism set included gas phase reactions and also a reaction where K_2SO_4 condensates which is an irreversible reaction. This mechanism has not yet been proved to be valid but has worked good to describe previous studies well. The mechanism set includes only potassium, but other metals from the biomass ashes may also interact with sulfur and the radical pool, which is not studied in this project.

Chemkin has an inbuilt tool that can perform a parameter study. It performs modelling of the whole reactor with the same parameters except for one, which is varied for different runs. With this tool, different inlet specie concentrations could be studied and sensitivity analyses were made for temperature and dimensions of the reactor, varying one parameter at a time. The parameter study can also be performed varying two parameters at a time. In such way, temperatures could be varied with a specie fraction of sulfur representing both the fraction with and without the sulfur addition. Thereby, it could be investigated at what circumstances the case with sulfur addition was favourable in terms of CO oxidation.

The reaction rates in the models were investigated by both plotting and integrating. The important reactions were integrated over the whole reactor and compared to see which ones are dominating and to identify differences between different operating conditions. The reaction rates were given in Chemkin as mole/cm^{3}s and when integrating over residence time, the unit was mole/cm^3.

3.2.2 Modelling procedure

The procedure of the modelling will be explained here and it was not determined on beforehand but rather due to the results the previous models gave and what answers they still left unanswered. First the 3 equilibrium models are presented and then the 6 models of the PFR reactor are presented. It was mainly CO outlet concentration and reaction rates that was investigated for different inlet conditions of K/S/Cl species, temperatures, residence times and equilibrium studies.

In Table 3.1 the specie fractions and temperatures for the equilibrium models are presented. The equilibrium between potassium, sulfur and chlorine species were investigated in order to show how they were likely to be present in gas phase in the boiler. Data for the main components in the gas phase were taken from the experiments as inlet data but the uncertainties around the amounts of Cl, K and S made it difficult to know the exact inlets. The first equilibrium model used an excess of sulfur and chlorine compared to potassium in order to see what potassium is most likely to form if there are no restrictions on other species. The model was made for a large temperature span of 700-1400 °C since the equilibrium is very temperature dependent. It was also studied how the equilibrium between chlorine species varied

with temperature with these inlets. The second equilibrium model used an excess of potassium and chlorine in order to see what sulfur was most likely to form with no restrictions for other species. Finally a model was made with the initial conditions that was obtained from the experiments, with a varying temperature over a smaller span of 750-1000 °C. The temperature was narrower since the temperature was known in the experiments.

Table 3.1: Table of K-Cl-S species and temperatures in the different equilibrium models. Specie fractions are presented in ppm and temperatures in °. Equi 3 is shown in the section comparing the experiments with the modelling.

Model	**K**	**Cl**	**S**	**T**
Equi 1	200	300	300	700-1400
Equi 2	300	300	100	700-1400
Equi 3	65	8.4	8.9, 33.7	750-1000

In Table 3.2 the inlet specie fractions of K-S-Cl, residence time and temperatures are shown for the models presented in the report. The first models of the PFR reactor were made to investigate the relation between potassium and sulfur and how they interacted where chlorine was neglected. It was assumed that sulfur was most likely to be present as SO_2, which always was used as the sulfur inlet specie. From previous literature it was suggested that potassium and sulfur form K_2SO_4 and its reaction mechanisms were also crucial for these models to study. The first model on this subject was varying KOH inlet with 4 different SO_2 inlets. How the fractions K, KOH, K_2SO_4 and OH was varied throughout the reactor was also investigated at interesting potassium and sulfur SO_2 fractions. These species were necessary to study since they were expected to be responsible for the effect of KOH excess on CO oxidation. A new model was made by instead varying SO_2 at a constant fraction of KOH. That model was further investigated by studying the reaction rates to understand the behaviour of the concentration differences that occurred. The reaction rates were investigated throughout the reactor for different SO_2, and therefore different 2S/K fractions.

Table 3.2: Table of K-S-Cl species, temperatures and residence time at the inlet of the different models. The specie fractions are shown as ppm. K/S represents the models where only K and S was varied. τ,T represents the models where residence time and temperature was varied. Cl represents the models where the influence of chlorine was studied.

Model	**KOH(ppm)**	**KCl(ppm)**	**HCl (ppm)**	**SO_2(ppm)**	**τ(s)**	**T(°C)**
K/S 1a	0-300	-	-	0,20,40,60	0.64	790
K/S 1b	50,90,170,250	-	-	40	0.64	790
K/S 2a	300	-	-	0-200	0.64	790
K/S 2b	300	-	-	85,105,125	0.64	790
τ,T a	300	-	-	0-200	0.32	810,830,850
τ,T b	300	-	-	50	0.32	810,830,850
Cl 1a	300	0,50,100,150	-	0-200	0.64	790
Cl 1b	300	0,100	-	150,180	0.64	790
Cl 2	150-300	0-150	-	0-200	0.64	790
Cl 3	300	-	0-150	0-200	0.64	790

The effect of temperature and residence time were then studied with the same inlet specie fractions making it easier to compare with the base case. Since both parameters are rather uncertain and can be various for different types of boilers this was crucial to investigate. Previous models used a temperature of 790 °C and a residence time of 0.64 s. The temperature however is a lot higher in the combustion chamber of the experiments and therefore a higher temperature was investigated. The residence time may vary very much since the SO_2 may be injected in many different positions and the boilers have many different sizes and flows. It was suggested that the reactions would take place instantaneously in the reactor and therefore not be significantly dependent on residence time, which was studied by both increasing and decreasing residence time. The presented model was made to show how the effects on CO oxidation by increased temperature and decreased residence time.

Chlorine in shape as KCl was then introduced to the reactor inlet, varying SO_2 and having a constant KOH fraction as before. The reactions were then studied in order to understand how the KCl addition affected the radical pool and also the combustibles reaction paths. The study compared cases with 0 and 100 ppm KCl at 150 and 180 ppm SO_2, since that was the interesting points to study. Another model was also made when the potassium content was constant but divided differently between KCl and KOH. The total K fraction was always 300 ppm but was divided between KCl and KOH. These cases were compared with a model of different KOH contents without KCl. Having chlorine released as HCl was also studied and compared with the other models.

3.3 Comparison between experiment and modelling

In order to create an environment to the modelling close to the one in the boiler, specie compositions and other operating conditions were collected from the experiments. The specie fractions were calculated with both measured data and together with the fuel report. The dimensions of the boiler were estimated with the help of drawings of the boiler. The part of the boiler which was interesting to dimension was from after the cyclone to the convective pass. This part was chosen since it had been observed that sulfur addition from the top of the cyclone made CO decrease and since the convective pass cools the flue gas down, it was not necessary to model further.

The purpose with this model was to represent the environment and specie fraction compositions from the experiments made in the CFB boiler and to model how the combustion occurred after the cyclone. The model had as a goal to create a scenario where CO outlet concentration was lower when sulfur was injected, maintaining the running parameters as much as possible. Together with trends from the earlier models it could be estimated what would happen with the model if any parameters would change. The inlet SO_2 fractions were kept at 9 and 34 ppm as the calculations from the experiments suggested.

4

Results

4.1 Evaluation of experiments

The experiments had similar operating conditions but different injection strategies which is why they have been separated into continuous and batchwise addition. For all experiments, operating conditions such as gas velocity, fuel flow and air flow were kept constant and will only be presented in order to provide data for the modelling. A large focus on the results is put on S and CO since K and Cl species were not measured.

4.1.1 Influence of continuous sulfur feeding

Figure 4.1 shows concentration of CO in the chimney and it can be seen that after the start of sulfur feeding the CO goes down to zero and keeps there during the remaining operation. The CO concentration before the sulfur feeding is fluctuating but can be approximated to have a concentration of around 150 ppm. From the point where sulfur was fed, it took about 20 minutes until most CO was gone and 45 minutes until all was gone in the chimney. That may be due to that the sulfur dosing was small and that the return flow from the cyclone to the combustion chamber makes it slow for the system to adjust.

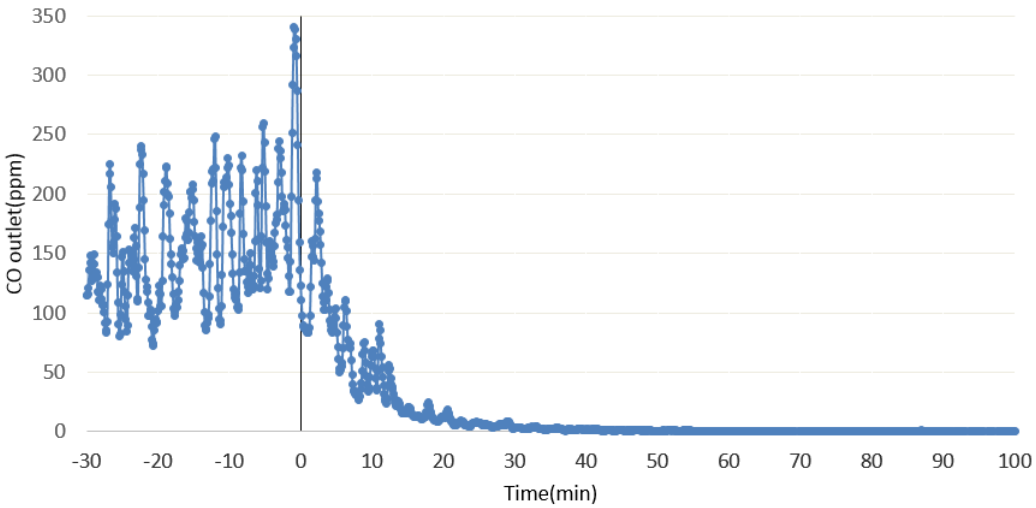

Figure 4.1: CO concentration in ppm in the chimney vs time in minutes. Sulfur feeding was started at time 0.

Figure 4.2 shows concentrations of O_2, CO_2 and CO in H12 before and during the sulfur feeding. The level of CO_2 increased and the level of CO and O_2 decreased during the sulfur feeding. These figures makes it reasonable, but not evidential, to say that the sulfur feeding makes CO and O_2 to form CO_2. However, only about 1/3 of the CO in H12 was decreased by feeding sulfur. Compared to the chimney, these results show that the oxidation of CO has started in the combustion chamber but the full oxidation occurs further downstream the boiler. CO and CO_2 are lower on the left side than the right side whereas O_2 has the opposite behaviour. That might be due to combustion chamber characteristics.

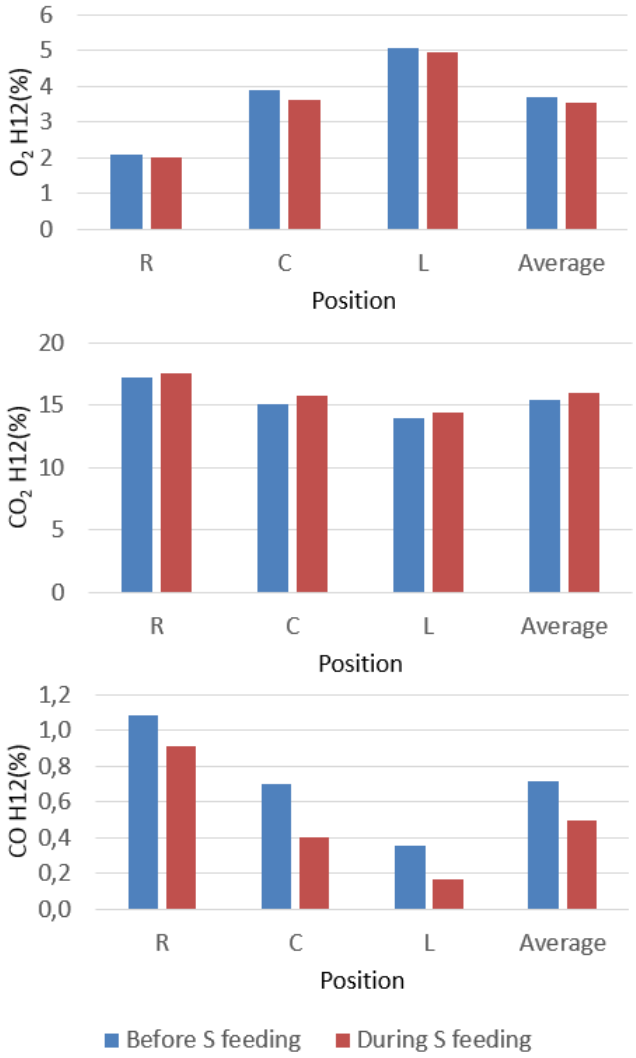

Figure 4.2: CO concentration(%) in H12 positions before and after the start of sulfur feeding. R=Right, C=central, L=left side in the chamber.

Figure 4.3 shows SO_2 and CO concentration at the time were sulfur was started to be fed showing that SO_2 increases after CO reaches its bottom level. From the point where sulfur was fed it took about 70 minutes until SO_2 started to increase and CO about 45 minutes to reach 0. During the 35 minutes where CO is at bottom level and SO_2 do not increase, it can be suggested that the fed sulfur was formed into

something else than SO_2, or from SO_2 into something else. After 70 minutes, the system had that much sulfur that the system was saturated with SO_2 and an excess of SO_2 was created which may be due to the recirculation in the CFB boiler.

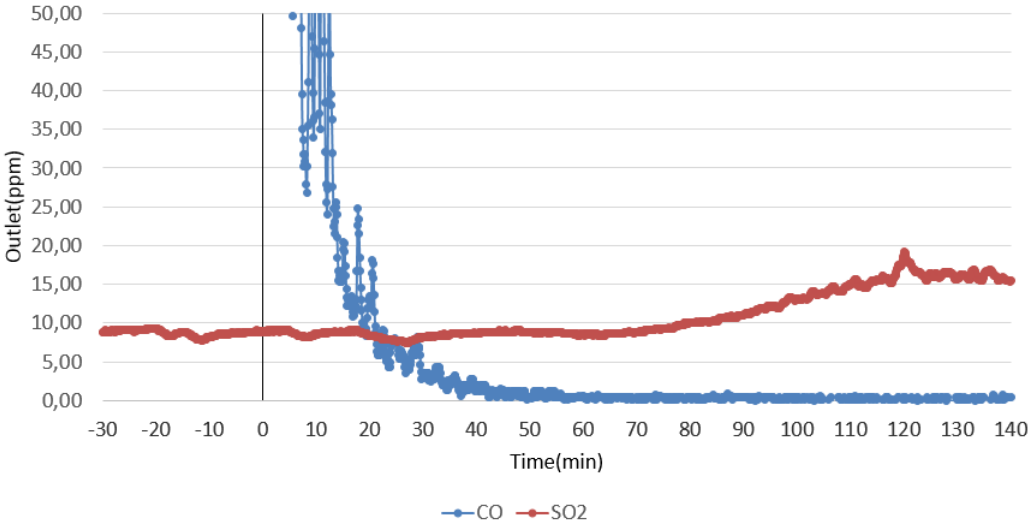

Figure 4.3: SO_2 and CO concentration in ppm in the chimney vs time where 0 is the time when sulfur injection was started. The blue is CO and the red is SO_2.

Table 4.1 shows the sulfur flows at both inlet and outlet and is compared by the conversion. The inflow consisted of sulfur from both the sulfur in the fuel and from the feeding. From the table it can be seen that the conversion of sulfur was higher before the sulfur feeding which means that the sulfur in the biomass was present as SO_2 in the outlet in a larger share than the sulfur coming from during the additional sulfur feeding. The SO_2 outlet flow was, however, larger during the sulfur feeding but in total, less percentage was reacted to SO_2. The sulfur that was added through feeding may therefore have been present as K_2SO_4 or got caught in the boiler. Quality of the measurements is a factor that makes these values hard to fully trust.

Table 4.1: Table of detected SO_2 due to the sulfur feeding. The mass of SO_2 is then translated into mass of sulfur, which eventually can be used to calculate the amount of sulfur that was detected as SO_2 compared to the amount of sulfur that was inserted.

Time slot	**Inflow S (kmol/h)**	**Outflow SO_2 (kmol/h)**	**X, S to SO_2 (%)**
Before S feeding	7.54	3.13	41.51
During S feeding	44.96	7.02	15.61
Due to S feeding	37.41	3.89	10.40

Table 4.2 investigates the behaviour of sulfur in H12. It can be seen that the highest conversion of the inlet sulfur to SO_2 in H12 was highest without sulfur feeding, as in the table above. During the sulfur feeding the conversion is about 50%. However, comparing this table with Table 4.1, it can be seen that in all cases the SO_2 fraction

is larger in H12 than in the outlet. That implies that SO_2 is further reacted since it is not probable that SO_2 get stuck in the reactor. It can also be possible that all sulfur was formed into SO_2 at some stage before H12 and some formed into new species before H12. Due to the high temperature and good mixing, it is reasonable that all sulfur was formed into SO_2. The reason why more SO_2 was consumed after H12 than before may be due to that the flow was better mixed in the cyclone, that the reactions were favoured by lower temperatures or that the reactions were slow and thus needed more time. One reason may also be that before H12 there were more volatile species that used all reactive radicals, whereas after H12 more radicals than volatiles were present giving SO_2 a chance to react with the radicals.

Table 4.2: Table of SO_2 in H12 and conversion of S from the inlets to SO_2 in H12.

Time slot	H12 flow SO_2(mol/h)	Conversion(%)
Before S feeding	5.08	67.37
During S feeding	22.31	49.62
Due to S feeding	17.23	46.05

The temperatures in the systems were mainly kept constant, but Figure 4.4 shows the temperature in the combustion chamber. The plot shows that the temperature in the top of the bed was fairly constant but the temperature increased at the bottom after sulfur feeding. The temperature increases during a time span of 50 minutes and the total rise is about 6.86 °C. The rise may be due to oxidation of sulfur into sulfur dioxide in the bottom. However the temperature rise is very high compared to the small amount of sulfur that was injected.

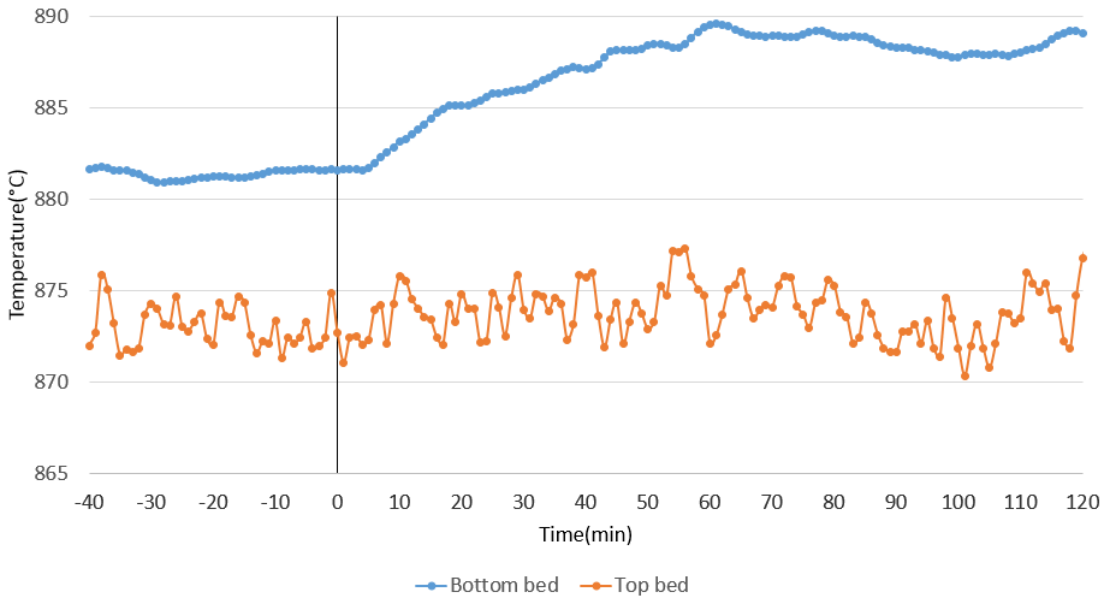

Figure 4.4: Temperatures(°C) in the combustion chamber for the top and bottom of the bed vs time in minutes. Time 0 is when the sulfur injection started.

By making a quick heat balance over the system, it was found that this temperature

increase was equivalent to approximately 27 kW of heat increase. If all of the sulfur injection of 1.2kg/h oxidised instantaneously at the bottom of the bed, it would represent a heat release of about 3kW. Consequently, a heat increase of 3kW represents a temperature increase of 0.8 °C which would be difficult to observe. That suggests that it was not only the sulfur oxidation that contributed to the temperature increase. However, there are no visible temperature rise at the top of the bed, meaning that the same amount of heat released from reactions have taken place at the top of the bed. It is therefore most likely that inside the combustion chamber, the sulfur injection shifted the main combustion in a way that more reactions took place in the bottom of the reactor than without the sulfur feeding.

Figure 4.5 shows the temperature for four different measurements after the cyclone. Contrary to the bottom of the boiler, all measurements after the cyclone shows that the temperature goes down when sulfur is injected. It is reasonable that probe A and B gives higher temperature due to that they are put upstream to probe C and D. The temperature drop is on average 5.18 °C. By making a similar heat balance as for the temperature increase in the bottom of the bed, this temperature decrease is equivalent to approximately 20 kW. By removing the 3 kW from the 27 kW as the oxidation of sulfur stands for, the heat increase at the bottom of the bed is almost equal to the heat decrease in the top of the cyclone. That suggests that the overall combustion process is shifted in a way that more reactions occur at the bottom of the bed and less in the top of the cyclone. It may also be possible that the temperature drop is due to the condensation of K_2SO_4 which might form at this point in the boiler.

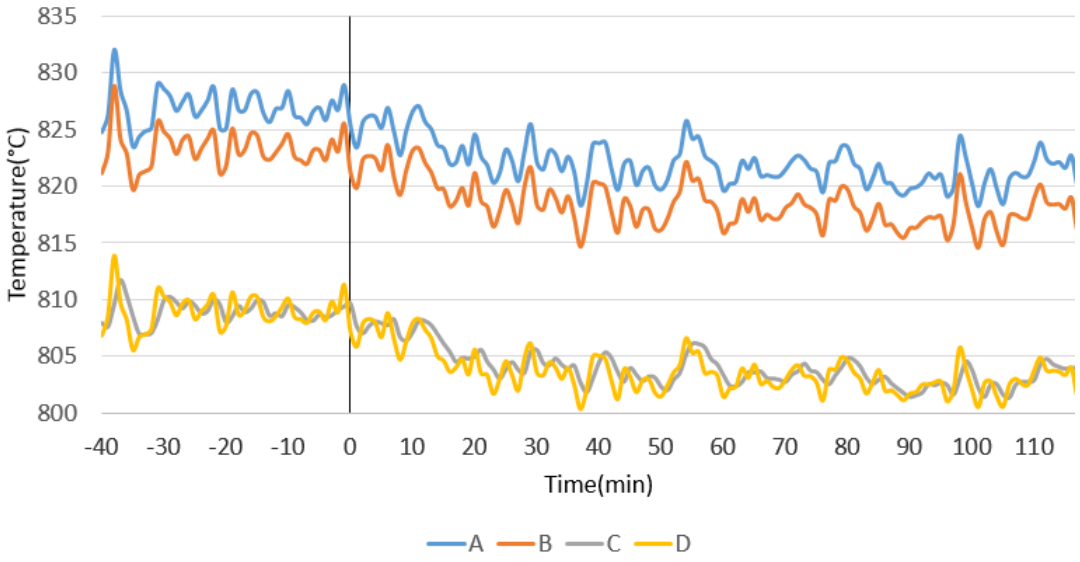

Figure 4.5: Temperatures(°C) after the cyclone for 4 different measurements vs time in minutes. Time 0 is when the sulfur feeding was started.

Table 4.3 shows how the concentration of carbon species changes throughout the boiler. Most of the carbon was present as CO_2 in H12. 85-86% of the total conversion of carbon to CO_2 was already made in the combustion chamber. However, there

were much CO left in H12 left, meaning that a lot of CO consumption was made downstream the combustion chamber. The CO concentration was quite high in H12, both before and during sulfur feeding. Comparing the molar flow of CO in H12 before and during sulfur feeding it can be seen that roughly 0.82 kmol/h was reduced and for CO_2 the molar flow was increased by 0.76 kmol/h. That observation suggests that the reduction of CO during sulfur feeding is found as CO_2 instead.

Table 4.3: Table of carbon species in different positions in the boiler. The conversion shows how much of the carbon from the fuel that is present as CO and CO_2 in H12. The CO and CO_2 was measured in H12 and outlet before and after sulfur feeding.

Specie	**Inlet(kmol/h)**	**Conversion**	**H12(kmol/h)**	**Outlet(kmol/h)**
Carbon species	50.75	-	-	-
CO before	0	4.78%	2.42	0.05
CO_2 before	0	84.73%	43.00	50.93
CO after	0	3.16%	1.60	0
CO_2 after	0	86.23%	43.76	51.30

4.1.2 Influence of batchwise sulfur addition

In Figure 4.6 the concentrations in H12 are shown at conditions between the sulfur additions. From the figure it can be seen that the concentrations are rather evenly distributed, which is the purpose of the CFB boiler. The point where most deviation from other points can be seen is B:L, which is where the gas flows back from the return pipe further down in the combustion chamber. That deviation is therefore due to chamber characteristics and thus not chemistry characteristics. The figure also shows that SO_2 mostly follows the trend as CO and CO_2, meaning that SO_2 is low where O_2 is high.

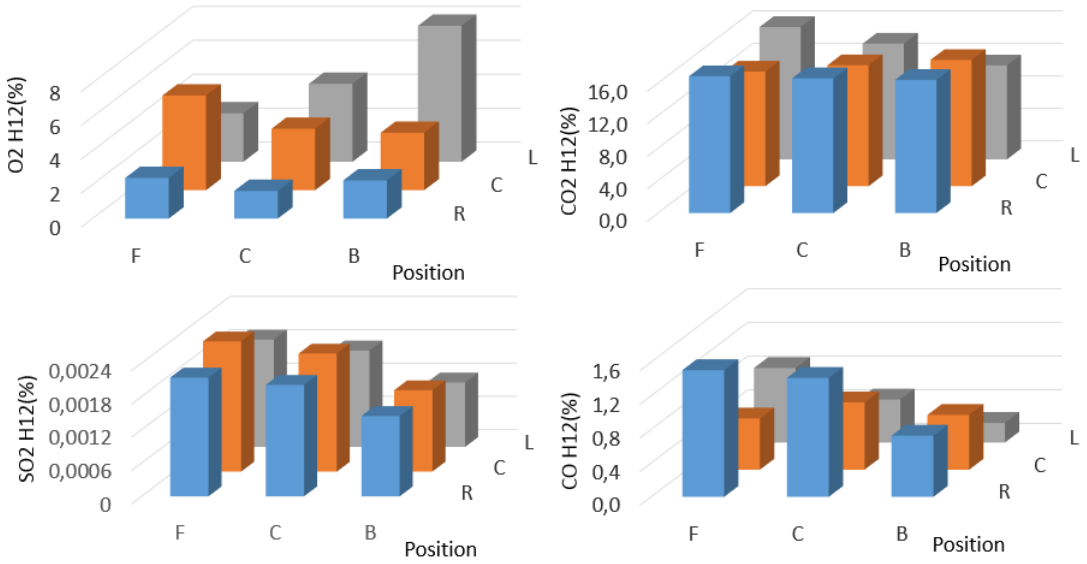

Figure 4.6: Concentrations(%) for species in H12. Upper left is O_2, upper right is CO_2, lower left is SO_2 and lower right is CO. F=Front(where the fuel is injected), C=centrum, B=Back, R=Right and L=Left

Figure 4.7 shows the CO and SO_2 concentration detected in the chimney during the six sulfur additions. The figure shows clearly that in the four first additions the CO concentration goes down to almost zero at the same time as SO_2 is detected above its normal level. Since less sulfur was added in the first addition, less SO_2 is detected in the chimney, although the CO is decreasing to close to 0. The figure shows that the peak of SO_2 in the chimney is detected after 2-4 minutes and it takes a little less than one minute from the first SO_2 to be detected until the maximum point of SO_2 is detected. The two last additions which were inserted in the return pipe however, does not give any significant amount of SO_2 nor decrease of CO in the chimney. The figure also shows how the CO decreases completely after the continuous sulfur dosing was started, which was made two minutes after the fifth sulfur addition. It is therefore difficult to draw conclusions from the two last additions but it seems like the CO concentration is not significantly affected by the additions but rather to the continuous feeding. From observation in H12 it was known that most of the fuel sulfur is present as SO_2 in H12. It is therefore reasonable that the sulfur from the additions where sulfur was added from the return pipe also should be present as SO_2. However, no change in SO_2 in H12 was observed and six minutes after the last addition, SO_2 was actually decreased in H12.

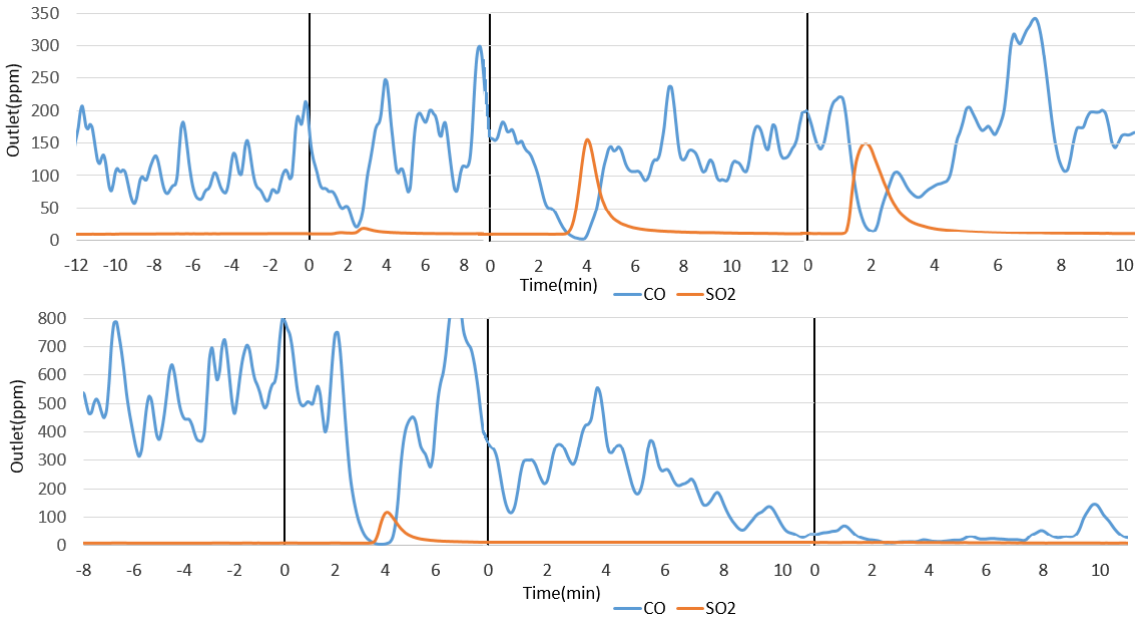

Figure 4.7: CO and SO_2 concentration(ppm) vs time in minutes during the occasions when sulfur was added. The x-axis is related to when sulfur was added.

These graphs made it possible to calculate how much sulfur that was detected in the chimney. The results are found in Table 4.4, where the second, third and fourth addition were considered. Addition 2 and 3 gave a slightly higher SO_2 detection in the chimney than addition 4 and one difference between these additions were that CO was present in a higher extent(around 200 ppm for 2 and 3 and around 500 for 4). The remaining sulfur may then be present as un-reacted sulfur or as further reacted into K_2SO_4.

Table 4.4: Table of detected SO_2 after sulfur additions. The mass of SO_2 is then translated into corresponding mass of sulfur, which was used to calculate the fraction of injected sulfur detected as SO_2 in the chimney.

S Addition number	**Mass SO_2(g)**	**Corr. mass S(g)**	**Conv. of S to SO_2(%)**
2	53.91	26.98	31.75
3	59.05	29.56	34.77
4	40.14	20.09	23.64

4.2 Modelling of combustion chemistry

In this section, the results from the modelling will be shown and discussed. Reaction numbering is referred to the theory section where the reactions have been introduced, which will be necessary to go back to in order to understand the discussion in this section. The inlet fractions of the major species was taken from the experimental results, shown in Table 4.6, and was used throughout the modelling in order to have

similar environments as in real combustion of biomass in CFB boilers.

4.2.1 Chemical equilibrium calculations

Equilibrium calculations were made in order to study how the K-S-Cl species were likely to be present at chosen operating conditions. In Figure 4.8, equilibrium fractions of KCl, KOH and K_2SO_4 was plotted against temperature. The figure shows that around 800 °C almost all K is released as K_2SO_4 and a minor fraction of KCl. At higher temperatures K_2SO_4 decreases whereas KCl increases and it takes until 1100 °C until KOH starts to form in the equilibrium calculator. However from the experiments, it was shown that the temperature does not exceed 900 °C and thereby it can be concluded that KOH will not form when there is Cl or S present.

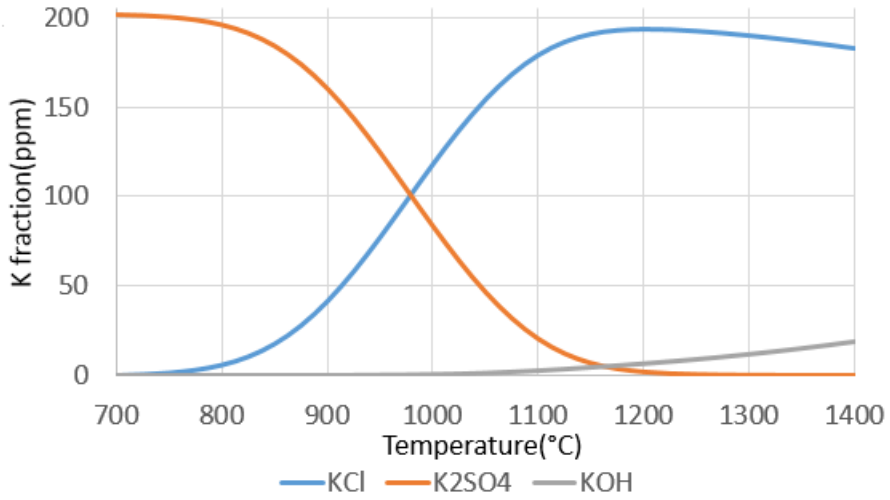

Figure 4.8: Equilibrium fractions for KCl, KOH and K_2SO_4 vs temperature with 200 ppm K at the inlet. The plot is adjusted for K_2SO_4 so that each mole of K_2SO_4 is shown as 2 moles since it hold two moles of K. Blue is K_2SO_4, red is KCl and grey is KOH.

The chlorine species were studied with the same operating conditions as above. The equilibrium is presented in Figure 4.9. Since 200 ppm Cl was set as the inlet, the figure shows that all chlorine always is present as HCl or KCl. At lower temperatures KCl is dominating but around 1040 °C and above HCl is dominating.

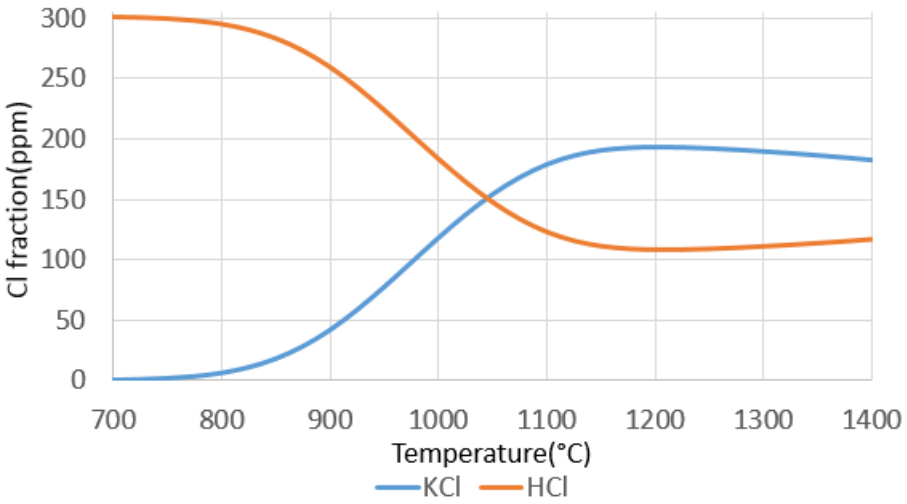

Figure 4.9: Equilibrium fractions for KCl and HCl vs temperature with 200 ppm Cl at the inlet. Blue is KCl and red is HCl.

4.2.2 Influence of sulfur and potassium

A model, shown in Figure 4.10, was made in order to investigate how sulfur and potassium affected CO oxidation. KOH inlet was varied for different amounts of SO_2 inlets, everything else was kept constant and no chlorine was present. The first figure shows that all SO_2 fractions have similar trends. When KOH is in excess the CO concentration decreases until an optimal point, where CO concentration then increases. As long as the KOH content is lower than twice the amount of SO_2 the CO concentration is around 109 ppm. The second plot in Figure 4.10 was made to visualise the trends observed. The cases with different SO_2 inlets shows a very distinct trend when twice the amount of inlet SO_2 is subtracted from the KOH inlet. The reason for this behaviour is that all SO_2 forms K_2SO_4 when potassium is available. Thus, this figure suggests that it is only excess KOH that affects CO oxidation.

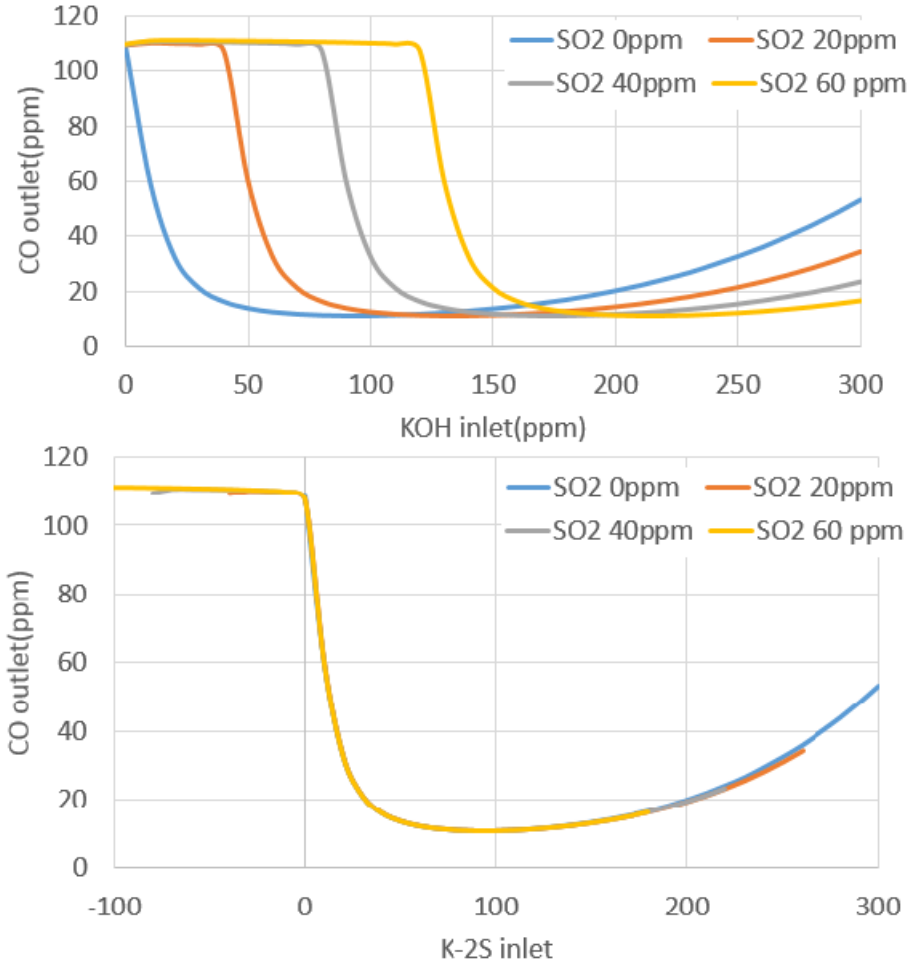

Figure 4.10: CO outlet concentration vs inlet concentration of KOH in the first plot and the difference of inlet KOH minus 2*inlet of SO_2 in the second plot. The plots are representing SO_2 inlet concentrations where blue is 0ppm, red is 20, grey is 40 and yellow is 60 ppm.

Figure 4.11 shows regions that was found in the modelling, depending on 2S/K ratios. Instead of plotting the inlet fraction of KOH inlet the 2S/K ratio is plotted giving a simpler way of explaining the regions. Region I is the part where the KOH inlet concentration is smaller than 2*SO_2 concentration which, evidently, do not affect CO outlet concentration. It was identified that at the transition between region I and II twice the amount of KOH was added in relation to SO_2. By observing the outlet concentration of K_2SO_4, it was discovered that in region I, all KOH was consumed to K_2SO_4. That reaction mechanism needs two K species for every S specie to form. Region II is the region where increasing KOH inlet concentration decreases CO concentration until a minimal CO outlet concentration is achieved. Region III represents where increasing KOH inlet concentrations increases CO outlet concentrations. In region II and III, all SO_2 forms K_2SO_4 but the remaining KOH is present in the outlet, only as an excess. However, from Figure 4.11, increasing amount of excess KOH decreases CO outlet in region II but increases CO outlet concentration in region III.

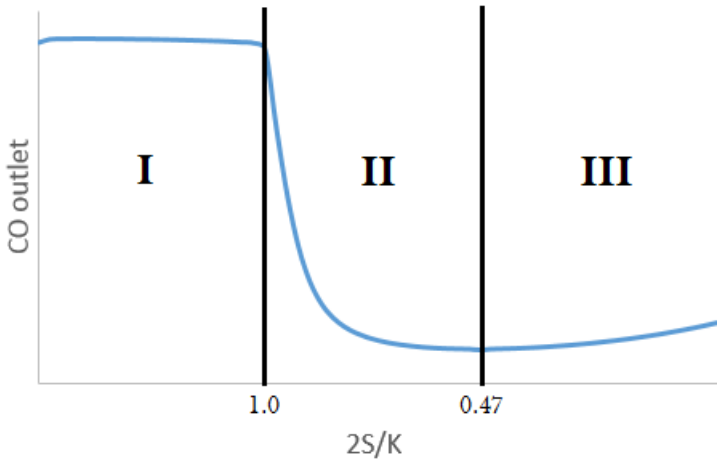

Figure 4.11: Presentation of regions for different 2S/K ratios. The graph shows CO outlet concentration vs inlet concentration of KOH(Decreasing 2S/K ratio). SO_2 was kept constant at 40 ppm and no Cl species were included. The x-axis in this plot is not increasing linearly.

In Figure 4.12 K, KOH, K_2SO_4 and OH were plotted inside the reactor for four different KOH inlets. The plots shows only the very first part of the reactor since that is where the most interesting fraction differences occur. KOH is first decreased as K_2SO_4 increased, which was expected. However, the fraction of K is also increasing at roughly the same time, especially for the regions with large KOH excess. The difference between the plots is that more K is formed with more KOH at the inlet, the plot with KOH deficit produces close to none K. Following the KOH and K line, they seem to interact with each other. This suggests that KOH is broken up to K and reacted back to KOH, together with the radical pool, which may be the reason why excess KOH affect CO concentration. However, observing the maximum point of OH, the less KOH injected the higher the maximum OH gets. Since the main reaction of CO to CO_2(Reaction 2.28) uses OH as a reactant, it would be intuitive to say that the case with largest OH fraction will yield the smallest CO outlet concentration. However, this study shows that the KOH inlet fraction giving optimum CO outlet has a maximum OH fraction when no KOH was in excess.

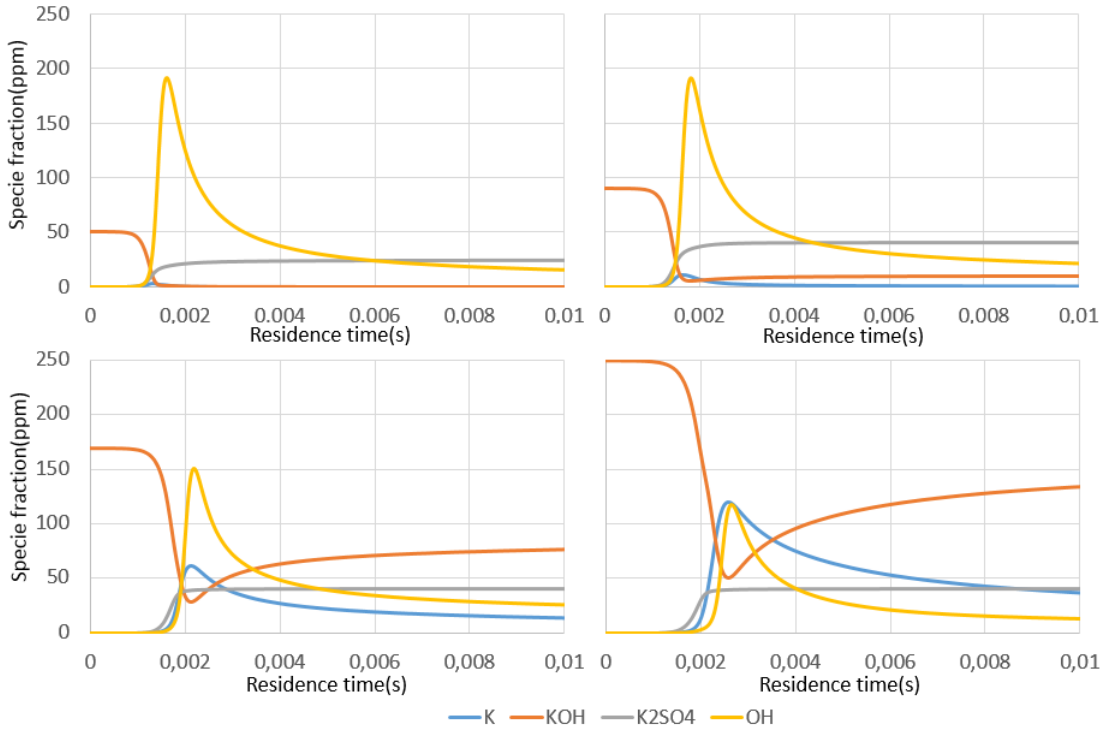

Figure 4.12: Fraction of species vs distance in the reactor. Blue is K, red is KOH, grey is K_2SO_4 and yellow is OH. All plots are from the case with 40 ppm SO_2 at the inlet. The upper left plot is for KOH inlet at 50 ppm, upper right at 90 ppm, lower left at 170 ppm and lower right at 250 ppm. This represents 2S/K fractions of 1.6, 0.89, 0.47 and 0.32 respectively.

Figure 4.13 shows the main reactions for KOH and SO_2 to form K_2SO_4. Figure 4.12 showed that K_2SO_4 was formed as long as there were potassium and sulfur and by observing the reaction rates, it was almost only the reaction path shown in Figure 4.13 that were present. The only deviation from this reaction path was that about 7% of the formed K_2SO_4 came from the reaction $KSO_4 + KOH \longrightarrow K_2SO_4$, as Reaction 2.27. A small fraction of KSO_3 is also formed from $KHSO_4$ but is directly formed back to $KHSO_4$, not affecting the overall reaction path. The reaction path with KO, KSO_3 and $KHSO_4$ showed not to be significant for the operating conditions in the model. The reaction path in Figure 4.13 consumes H and O_2 while forming H_2O and OH out of the O/H species. Region I, which represent various amounts of K_2SO_4 formation shows no change in CO oxidation. It is therefore suggested that the K_2SO_4 formation do not affect CO oxidation, even though it interacts with the radical pool.

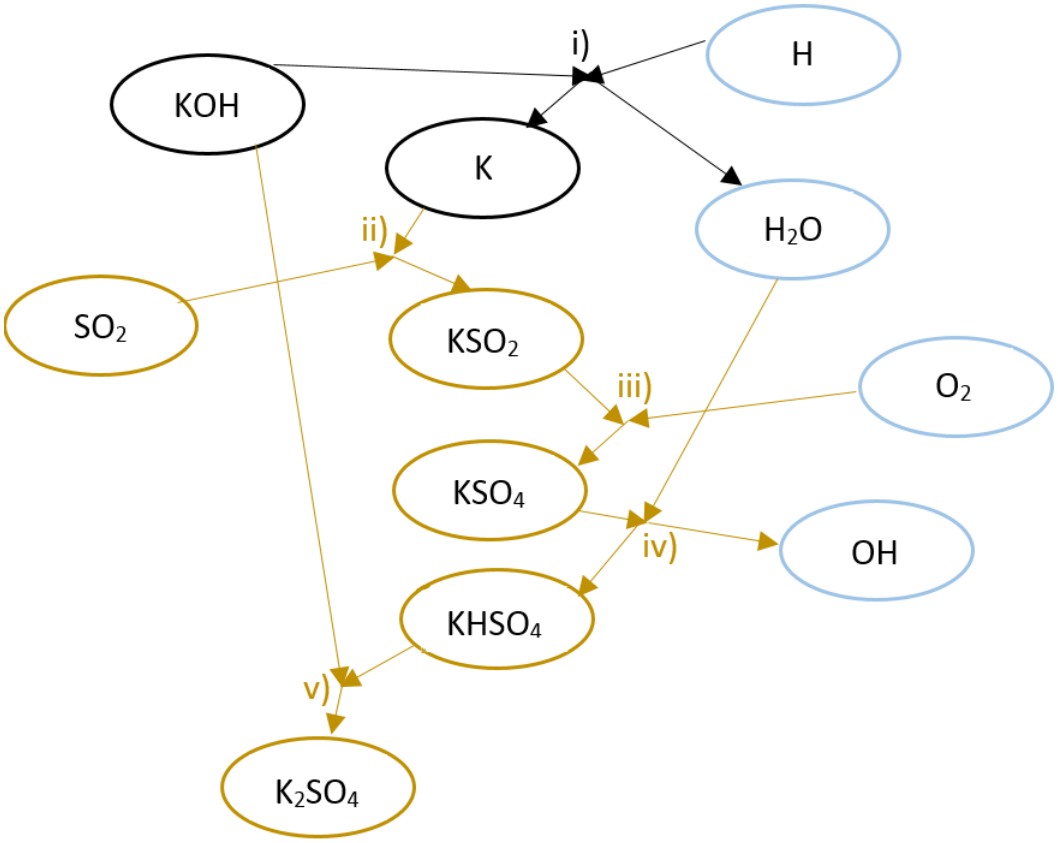

Figure 4.13: Visualisation of the main reaction mechanism forming K_2SO_4 from KOH. Yellow means sulfur involvement, black means potassium involvement and blur means O/H involvement. i) is reaction 2.13, ii) 2.23, iii) 2.24, iv) 2.25 and v) 2.26.

A new study was made, shown in Figure 4.14, with a constant KOH inlet of 300 ppm and varying SO2 from 0 to 200 ppm at a temperature of 790 °C. The CO outlet concentration follows a similar pattern as in Figure 4.11 and 4.10, but the regions are coming in the order III, II and I with increasing SO_2. Region III is from 0 to 0.68 2S/K, region II from 0.68 to 1 and region I from 1 and above. Once again, if there are not enough KOH to convert SO_2 to K_2SO_4 as in region I, the CO outlet concentration will not be reduced. It is thus the excess of KOH that is affecting the CO.

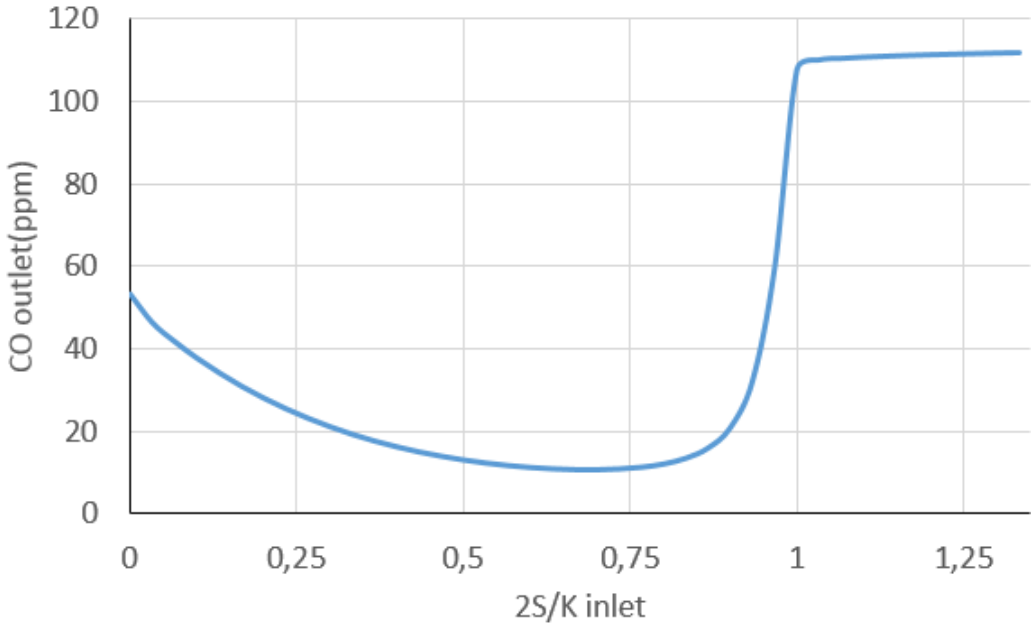

Figure 4.14: CO outlet fraction vs inlet quota of 2 SO_2 per inlet fraction of KOH. Inlet fraction of KOH set to 300 ppm and temperature constant at 790 °C.

From this study, reactions was further investigated in order to answer the questions why and how the excess of KOH is affecting the outlet concentration of CO. In Figure 4.15 three SO_2 inlets was investigated shown representing region III, between II and III(optimum in terms of CO oxidation) and region II. Following the CO concentration through the reactor it was discovered that the oxidation followed different paths with different excess of KOH. CO is mostly decreased in the beginning of the reactor, shown in the upper plots in Figure 4.15, but later in the reactor the decrease of CO occurs at significantly different rates affecting the total oxidation. In the early stage the case with low KOH excess is the most effective on decreasing CO whereas high KOH excess is decreasing less CO. In the later part in the reactor it is shown that the high KOH excess case is more effective on decreasing CO than lower KOH excess. This figure suggests that the case with 105 ppm SO_2(or 2S/K=0.7) has the best mix of CO decrease both in the early and late part of the reactor. These plots also suggests that the CO oxidation is dependent on reactions dominant in different parts of the reactor.

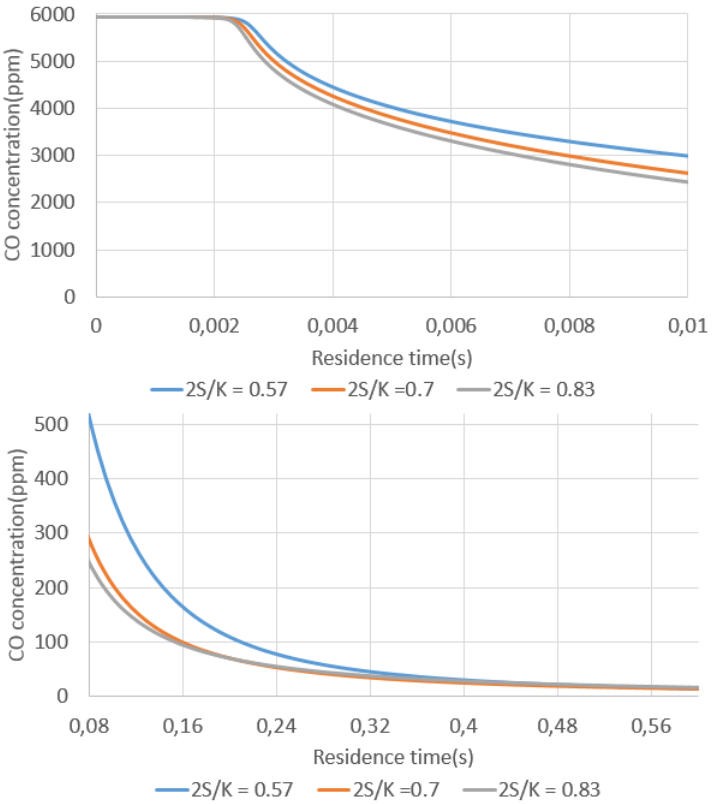

Figure 4.15: CO concentration(ppm) vs residence time(s) for different SO_2 inlets at different residence times. Blue shows 85 ppm SO_2 inlet representing region III(2S/K of 0.57), red 105 ppm SO_2 representing the optimum(2S/K of 0.7) and grey shows 125 ppm SO_2 representing region II(2S/K of 0.83). Temperature at 790 °C and KOH at 300 ppm.

In Table 4.5 integrated reaction rates of the CO_2 forming reactions from the same conditions as above are presented. It was fast concluded that all CO reacts into CO_2 and the reaction rates of CO_2 were therefore investigated. There are 5 reactions standing for almost all production of CO_2 which were investigated. The reaction rates were integrated verses the residence time in the whole reactor in order to determine how much each reaction occurred in total. Reaction 2.28a and b is the same reaction but the temperature exponent and activation energy for b is zero, meaning that its reaction constant equals the pre-exponential factor, which is much higher than for a. The table shows that Reaction 2.28a and b are dominating in all cases and these reactions are favoured by a low excess of KOH. In contrast to reaction 2.28a and b, Reaction 2.31 and on a smaller scale 2.32 is favoured by a large excess of KOH. However, Reaction 2.31 is small but the large difference between the cases of this reaction makes a significant impact on the total CO oxidation. There are thus no CO_2 forming reaction that peaks at the optimum KOH excess, it is rather the combination of two patterns that together yields an optimal CO outlet concentration.

Table 4.5: Table of integrated reaction rates(kmol/m^3) for the cases with different inlet fractions of SO_2 .

Reaction	2S/K 0.57	2S/K 0.7	2S/K 0.83
2.28a	37.116	38.4276	39.7167
2.28b	23.2918	24.1149	24.9238
2.31	6.2994	4.6189	2.7835
2.32	0.76842	0.37118	0.15254
2.30	0.65977	0.61132	0.53454
Total	68.1387	68.1482	68.1175

Figure 4.16 shows a chart of the main reactions affecting CO oxidation with altering KOH excess. There are many more reactions taking place, but the most crucial ones are presented here. These reactions have been investigated for different KOH excess and the evaluation is presented below.

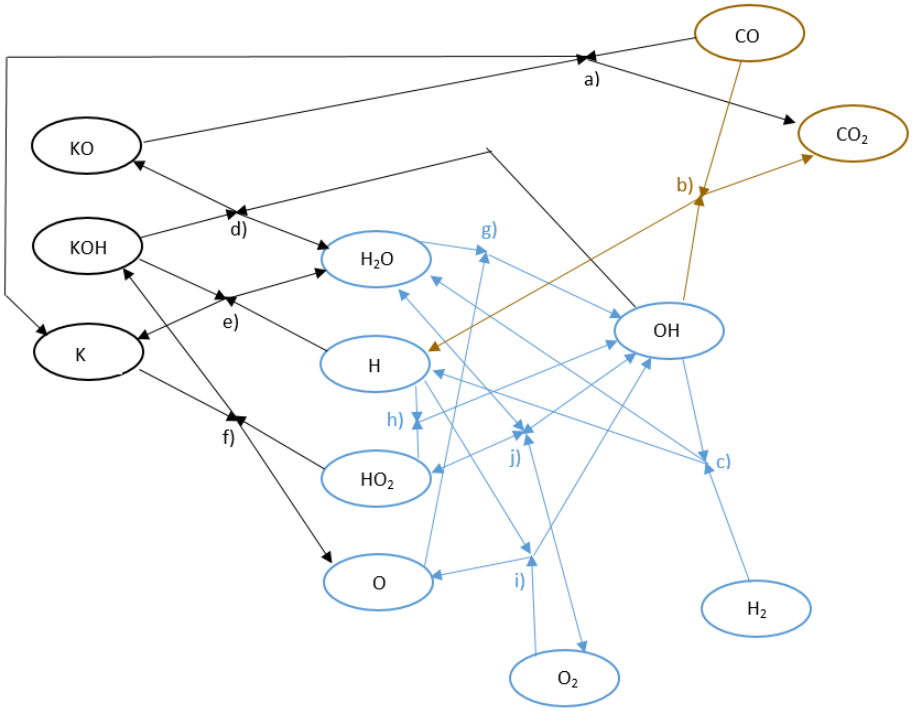

Figure 4.16: Reactions affected by KOH excess affecting CO oxidation. Black reactions includes potassium, yellow reactions includes carbon and blue reactions only includes O/H species. The arrows indicates if the specie is produced or consumed in the reaction. a) is Reaction 2.31, b) is 2.28, c) is 2.29, d) is 2.16, e) is 2.13, f) is 2.14, g) is 2.6, h) is 2.7, i) is 2.3 and j) is 2.8.

Large KOH excess had a relatively low CO oxidation in the early part of the reactor and a relatively high CO oxidation in the late part of the reactor. The patterns of early and late oxidation of CO will here be further investigated for different KOH excesses. In the early part of the reactor, reaction 2.28 dominates but is reduced by excess KOH, as seen in Table 4.5. Reaction 2.28 needs an OH radical, so it was

investigated if and why more OH radicals are formed in the early part of the reactor with low KOH excess. By observing the peaks of the reaction rates consuming OH, it was observed that Reaction 2.29 occurs at a much higher rate than 2.28a and b, which is a reaction oxidising H_2. It was known from before that oxidation of H_2 is much more reactive which these results proves. Reaction 2.8, which is terminating OH_2 into H_2O and O_2, is of equal order of magnitude as reaction 2.28a. Observing the peaks of the mechanisms forming OH, Reaction 2.7, 2.6, 2.3 and 2.8 are dominating. Reaction 2.7 and 2.3 both uses H to form OH and they are improved by low KOH excess, whereas Reaction 2.6 which uses O is reduced by low KOH excess.

The reactions of KOH were then observed for examining its contribution to the radical pool of H, HO_2, O and eventually OH. It was discovered that KOH was both consumed in Reaction 2.13 and later created once consumed by Reaction 2.14, probably since more KOH is available. There might therefore be some sort of equilibrium between reactions with radical species and KOH. The main KOH forming reaction is Reaction 2.14, which is forming O and consuming HO_2. The more KOH is in excess and makes Reaction 2.13 happen, the less H is available to Reaction 2.3 and 2.7 to form OH. To ensure that suggestion, H reaction rates were investigated and as observed before, reaction 2.13 is improved by increasing KOH excess consuming H. The oxidation of H_2 forming H is greatly decreased by increasing KOH excess and together with the increase of Reaction 2.13, reaction 2.7 and 2.3 are decreased. Reaction 2.4 is consuming H and forming HO_2 at a higher rate with small KOH excess and is the main consumer of H.

Observing the consumption of HO_2 it is seen that there is a shift as reaction 2.14 is the main consumption reaction in region II and Reaction 2.7 in region III. Reaction 2.14 is improved in region III due to that more K has formed and this reaction hinders the HO_2 to form OH in Reaction 2.7. To summarize the reason why a low excess of KOH is improving early CO oxidation in the reactor it can be said that the excess KOH will improve Reaction 2.13, decreasing H and HO_2, which decreases Reaction 2.3 and 2.7, which therefore is producing less OH which is the specie CO needs to form CO_2.

The second objective was to investigate why the later part of the reactor has improved CO oxidation with large excess of KOH. Once again, CO needs OH making the initial investigation to answer if and why more OH radicals are formed in the later part of the reactor with large excess of KOH. By observing the reactions forming OH, it is seen that in the later part of the reactor Reaction 2.6 is dominating where Reaction 2.6 and 2.3 are the only OH forming reactions that is improved by a large KOH excess. Reaction 2.6 is mainly improved since Reaction 2.14 occurs to a larger extent late in the reactor by higher KOH excess. The interesting fact that Reaction 2.3 is decreased by higher excess KOH in the early stage but improved in the later stage in the reactor may be since H is consumed by Reaction 2.13 at a greater extent with large KOH excess early in the reactor but not later. To summarize the argument that a high excess of KOH improves CO oxidation later in the

reactor is that more KOH makes Reaction 2.14 happen, which creates O that forms OH via Reaction 2.6. However, even though OH formation is improved later in the reactor by large excess of KOH, the total OH formation over the whole reactor is still decreased.

Looking on CO oxidation through the use of KO instead in Reaction 2.31 and in a smaller extent KO_2 in Reaction 2.32, it was observed that an increasing excess of KOH improves these reactions. When KOH excess is increased, the Reaction 2.13, forming K, is increased but also 2.16. Only 8% of the reactions consuming KOH comes from Reaction 2.16, the rest comes from Reaction 2.13. Reaction 2.16 uses an OH to form, but that OH loss is negligible in comparison to the total amount of OH reactions. However, when KO is formed it is directly consumed into K through Reaction 2.31. That reaction is though dominant in the later part of the reactor, using the OH radicals produced from Reaction 2.6.

4.2.3 Residence time and temperature dependency

The actual temperature during the combustion can vary a lot for different cases and boilers where also the uncertainty of the actual residence time made these two parameters important to vary. It was discovered that a lower residence time gave higher CO concentration. That was expected since the studies investigating influence of sulfur and potassium had proven that not all CO oxidation occur in the early stage, but that the later part also oxidises CO. It was the CO oxidation in region III that was most affected by reducing residence time which also was expected since region III has a larger share of its CO oxidation coming from Reaction 2.31 than in the other regions. Reaction 2.31 are, as mentioned earlier, more active later in the reactor than Reaction 2.28 making it more vulnerable to residence time.

Figure 4.17 shows a study made with temperatures of 810, 830 and 850 °C and half the residence time previously used. CO outlet concentration is plotted against increasing 2S/K ratio with the same KOH and SO_2 inlets as previous study, for simplification. Consequently, this study combined the trends of increasing temperature increases CO oxidation and decreasing residence time decreases CO oxidation. The figure shows how the CO concentration at very low 2K/S ratios in region III is higher than in region I, in contrast to the study with 790°C and normal residence time which had its maximum CO concentration in region I. At 810°C CO oxidation is still very favoured by small excess of KOH while at 850°C KOH excess is only worsen CO oxidation. At high temperatures CO oxidation is not dependent on Reaction 2.31 since most CO is oxidised by 2.28 in the early stage. The large difference of CO oxidation between the different temperatures in region I, where no KOH is in excess, shows how temperature dependent the CO oxidation through OH radicals are. The minimum CO oxidation is shifted towards smaller KOH excess as the temperature increases, by comparing 810 and 830°C. The actual minimum of CO is higher at 810°C for this case than in the case with 790°C and normal residence time. At temperatures low enough for an optimal CO oxidation, the optimal CO oxidation is residence time dependent.

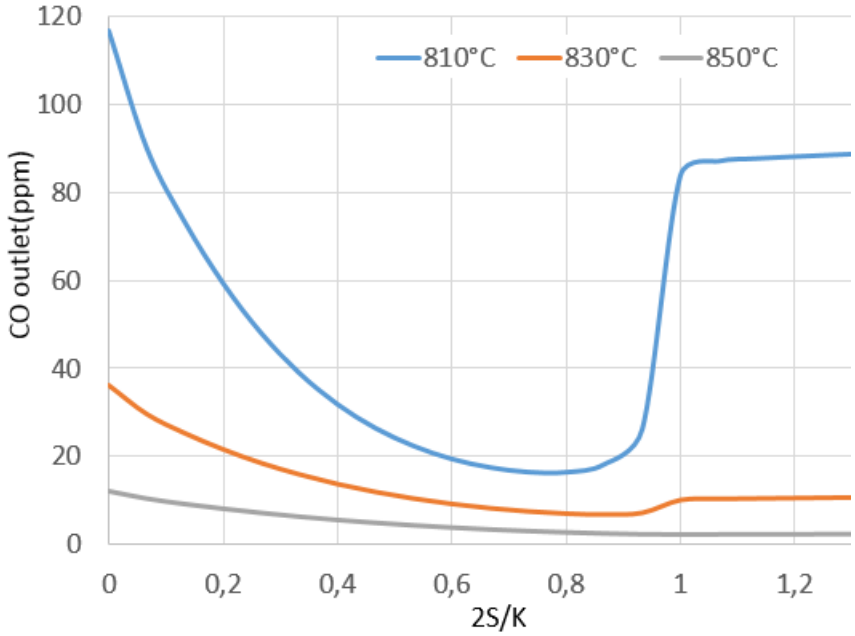

Figure 4.17: CO outlet vs 2S/K fraction. Blue has temperature 810 °C, red 830 °C and grey 850 °C.

The reactions forming CO_2 were investigated, but now for the temperature 810, 830 and 850°C at a 2S/K ratio of 0.33(in region III). In Figure 4.18 the same main reactions forming CO_2 are presented for the different temperatures in the very first stage of the reactor. The figure shows that Reaction 2.28a and 2.28b are clearly favoured by a higher temperature in the early part. The other reactions are also favoured by higher temperature but not as much. Since Reaction 2.28b not is temperature dependent but needs the OH radical, it suggests that the OH radical formation is clearly favoured by higher temperature. Late in the reactor however, all reactions are disfavoured by higher temperatures. That is probably due to that less CO and OH is available since it has already oxidised in the higher temperature case.

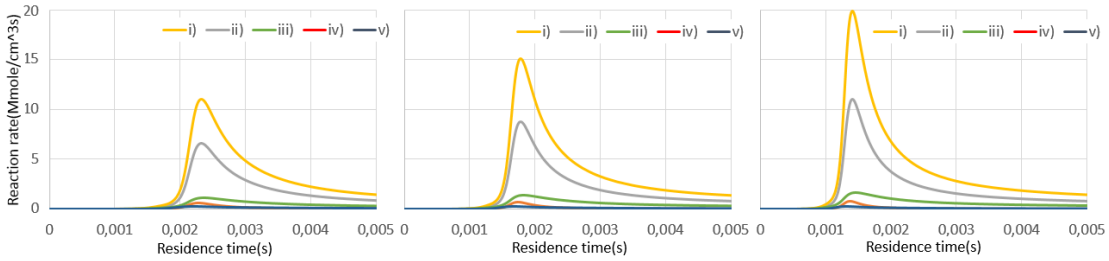

Figure 4.18: Reaction rates(Mmol/cm^{3}s) vs residence time at 810, 830 and 850 °C in the early stage of the reactor. i) is reaction 2.28a, ii) is 2.28b, iii) is 2.31, iv) is 2.30 and v) is 2.32.

4.2.4 Influence of chlorine

The small fractions of chlorine may affect the combustion chemistry and is investigated here. Figure 4.19 shows how the CO concentration for cases with different amounts of KCl and constant KOH at the inlet varies with SO_2. The figure shows that different KCl gives no difference in CO outlet concentration in region III and with SO_2 concentration around the optimal CO outlet. Then the pattern is that KCl improves CO oxidation at low KOH excess and high KCl excess(close to 150 ppm SO_2). When the KCl is in low excess, the cases including KCl actually decreases CO oxidation.

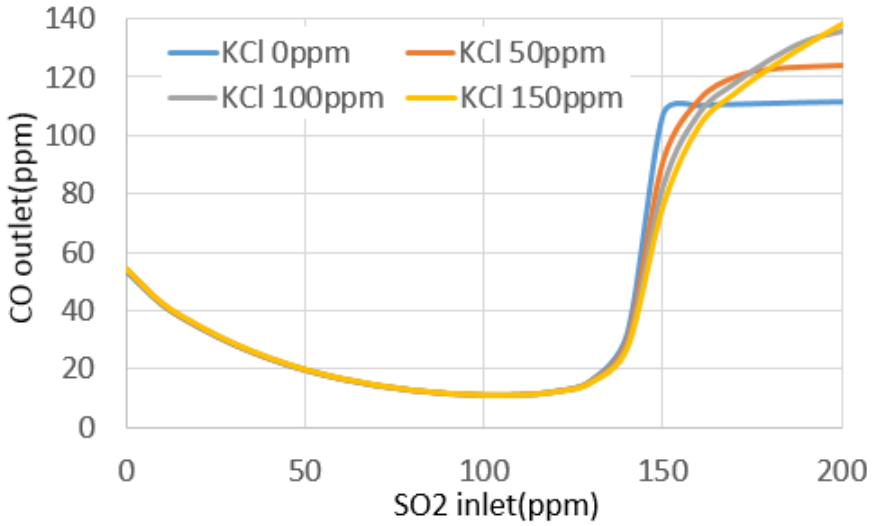

Figure 4.19: CO outlet(ppm) vs SO_2 inlet(ppm) for different inlet fractions of KCl. Blue has 0 ppm KCl, red 50, grey 100 and yellow 150. Inlet KOH kept constant at 300 ppm and temperature at 790 °C.

The regions where KCl does not affect CO oxidation will not be further investigated here, but the improved CO oxidation at 2S/KOH=1 and decreased CO oxidation at 2S/KOH>1 will be further investigated. A more thorough study was made with an inlet SO_2 concentration of 150 and 180 ppm and KCl inlet at 0 and 100 ppm. Firstly the case with 150 ppm SO_2 was studied where the CO oxidation was, as mentioned before, improved in the 100ppm KCl case. Observing the reactions that occur with KCl, it could be seen that KCl mainly goes into K and then back to KCl via Reaction 2.19. Some KCl also take part in the sulfation process forming K_2SO_4 but almost all Cl species are present as KCl or HCl and most forms back to KCl again via Reaction 2.20.

Observing the reactions forming CO_2 it is shown that about 99% comes from reaction 2.28, but there is also some of Reaction 2.31 present. In the case of 100ppm KCl, almost the same amount of reaction 2.28 is occurring but Reaction 2.31 is happening in a double amount. As known from before, Reaction 2.31 is requiring KO and is favourable in the later part of the reactor. This then suggests that the case with KCl at the inlet improves KO formation, preferably at the later part of the reactor.

The improvement of KO formation, however, is likely to come since KCl reacts with SO_2 giving more excess KOH that can form KO.

Observing reactions forming KO with the cases with and without KCl and most reactions are only slightly improved by the KCl case, but Reaction 2.16 is improved by more than twice of its total reactions in the case without KCl. Reaction 2.16 uses OH to form KO and all OH reactions were decreased in the case with KCl except Reaction 2.6. Both Reaction 2.16 and 2.6 takes place in the later part of the reactor which makes it reasonable to suggest that the increase of these reactions is the reason why Reaction 2.31 is increased in the 100ppm KCl case. From earlier explanations it was concluded that Reaction 2.6 was improved when H was consumed when KOH was in excess which increased O formation. In the same way reaction 2.20 is consuming H and therefore makes Reaction 2.7 happen less, which makes more HO_2 form more O through Reaction 2.14 and thereby more of Reaction 2.6 will occur. To summarize this reasoning it can be said that a case with KCl at the inlet makes more O to from, that makes more OH to form later in the reactor, which improves the KO formation and thereby the CO_2 formation from Reaction 2.31.

It was also investigated why CO oxidation was decreased at 180ppm SO_2. When 2S/KOH is larger than 1 , a very small fraction of Reaction 2.31 is occurring and can not help improvement of CO oxidation. However Reaction 2.28 is occurring slightly less with KCl than without. Since KCl is needed to form K_2SO_4, less of Reaction 2.19 and 2.20 occurs. However, these reactions do still happen and it uses a H, O or OH radical and forms H_2O as it goes into K, KOH and back to KCl. Therefore there are less radicals available for CO to oxidize and thus fewer reactions of Reaction 2.28 will occur.

An other model was made comparing different KOH inlet concentrations with and without KCl inlet concentrations. The inlet KCl concentration was either zero or the amount that was needed in order to keep total potassium concentration at 300 ppm. In Figure 4.20 the resulting CO outlet concentrations are plotted. The figure shows the same pattern as Figure 4.19, that KCl only influence CO oxidation when KOH starts to be scarce. At the interphase between region II and I, KCl slightly improves CO oxidation but later in region I KCl greatly decreases CO oxidation. Without going into detail on the reaction mechanisms it is assumed that similar explanations can be made here as in the previous model. When KOH is in excess, all reactions with SO_2 to K_2SO_4 uses KOH and thus KCl do not affect CO oxidation. When KOH is scarce, KCl interacts with SO_2 and a large excess of KCl improves CO oxidation whereas a small excess inhibits CO oxidation.

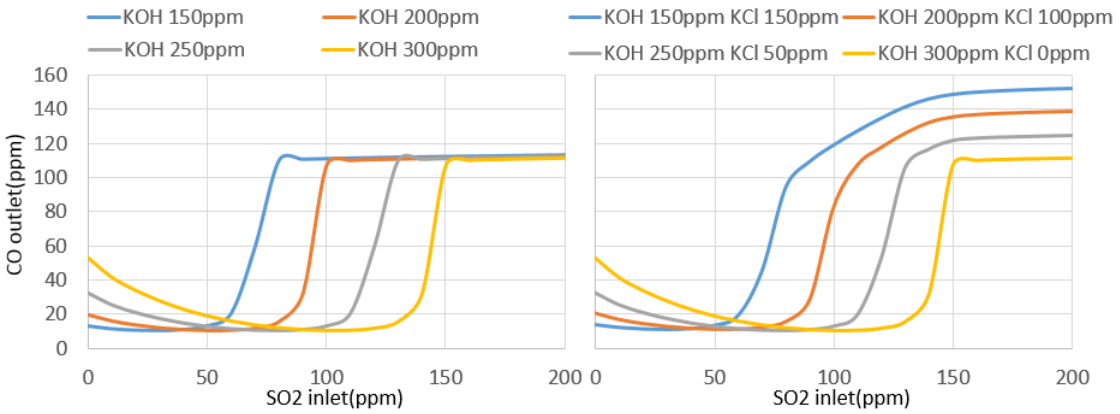

Figure 4.20: CO outlet(ppm) vs SO_2 inlet(ppm) for different inlet fractions of KOH and KCl. KOH concentration for blue is 150 ppm, red 200 ppm, grey 250 ppm and yellow 300 ppm. The left figure includes no KCl and the right figure includes KCl so the total amount of K is 300 ppm.

It is known that the chlorine in the fuel may be released as HCl instead of KCl and that there are an equilibrium between these species. This equilibrium and its affect on CO oxidation will be investigated and shown here.

In Figure 4.21 a study including HCl was plotted. KOH was kept constant at 300 ppm, temperature at 790 °C, normal residence time, varying SO_2 inlets from 0 to 200 ppm with different HCl inlets. No KCl was out at the inlet since this model represented a case when chlorine was released only as HCl. The figure shows a behaviour of CO oxidation as when KOH and KCl inlets were altered.

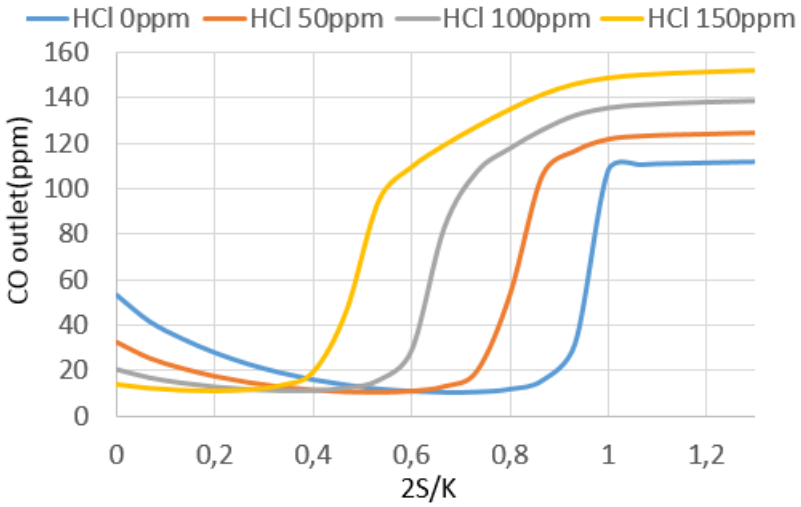

Figure 4.21: CO outlet vs SO_2 inlet for different inlet fractions of HCl. HCl concentration for blue is 0 ppm, red 50 ppm, grey 100 ppm and yellow 150 ppm.

Figure 4.22 is presented below and shows the outlet of KOH for different inlets of HCl. As HCl is added KOH is linearly decreased at the outlet. The reason for this behaviour is that HCl immediately form KCl and thereby uses one mole of KOH per

HCl to form KCl. By looking at the outlet concentrations of KOH when no SO_2 is added, where KOH can not sulfate, it can be seen that the outlet concentration is following an exact decline as HCl additions increase. The reason of this is of course that these modelled inlets is not in line with the chemical equilibrium that exists at these circumstances.

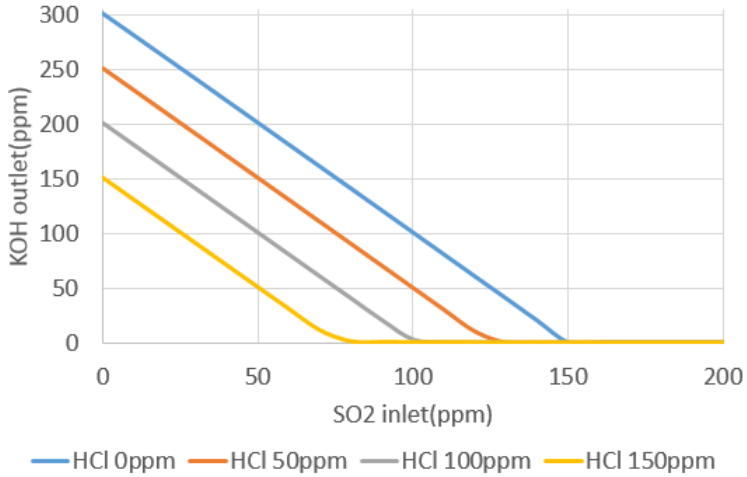

Figure 4.22: KOH outlet vs SO_2 inlet for different inlet fractions of HCl. HCl concentration for blue is 0ppm, red 50ppm, grey 100ppm and yellow 150ppm. KOH inlet was always 300ppm.

4.3 Comparison between experiment and modelling

In order to bring experimental and modelling results together comparison was made. Specie fractions measured, calculated and estimated from the experiments were used as inlets, trying to create a model that represented the results from the experimental outlets.

4.3.1 Parameter collection for the modelling

The length of the boiler was estimated from after the cyclone until the convective pass, where temperature decreases drastically and the reactions freezes. It was assumed that the reactor was a pipe and the corresponding diameter of this part of the boiler was measured and calculated to 1160 mm. The fuel flow was about 0.57 kg/s, the total air flow was about 2.37 kg/s giving a total mass flow of 2.94 kg/s. These values gave a residence time about 0.64 seconds, which has been used in the previous models as well.

The major species were kept constant in the modelling their calculated fractions are shown in Table 4.6. These values were taken from H12 in the boiler from the previous data evaluation. SO_2, KOH, KCl and HCl was also put at the inlet, but was changed

for the different models. When these species were inserted, the compositions of the constant inlet species decreased due to normalisation.

Table 4.6: Table of the specie molar fractions kept constant as inlets of the PFR in the modelling.

Specie	Inlet molar fraction(%)
CO	0.59
CO_2	11.64
H_2	0.90
H_2O	21.15
N_2	61.59
O_2	4.13

The fuel reports ultimate analysis indicated <0.02% of S and <0.01% of Cl species in the fuel which are values with a large uncertainty. A sulfur content imported from H12 and chlorine content of 0.01% in the fuel corresponded to a sulfur molar fraction of 8.9 ppm and a chlorine molar fraction of 8.4 ppm. When the sulfur feeding stream was added, the inlet fraction of SO_2 was increased to 34 ppm.

The ash content in the fuel was 0.53% according to the fuel reports ultimate analysis. In the ash analysis the potassium content were 15.1% and that corresponds to a total potassium content of 67 ppm in the boiler. These fractions are crucial for the modelling in order to re-create the behaviour of the experiments. Therefore it was necessary to vary these in the modelling.

Table 4.7 shows a summary over the inlet fractions used to represent the conditions in the experiments. KCl and KOH were kept constant as SO_2 was changed due to the sulfur feeding.

Table 4.7: Table of S, Cl and K molar fractions calculated from experiments that was used in the modelling.

Specie	Without sulfur(ppm)	With sulfur(ppm)
S	8.9	34
Cl	8.4	8.4
K	65	65

4.3.2 Equilibrium calculation of experimental fractions

Figure 4.23 shows equilibrium calculations where the experimental inlet fractions were considered and the resulting fractions are shown. The calculated fractions of inlet species from the experiment held less sulfur and chlorine than potassium as shown above. Both the case without sulfur feeding, holding 9 ppm sulfur and the case with sulfur feeding containing 34 ppm sulfur were studied. In the case without sulfur feeding, it shows that the same amount of Cl and S is present as

KCl and K_2SO_4 and the remaining potassium is present as KOH. In the case with sulfur feeding however, it is seen that almost all potassium forms SO_2 and KCl is only present in small fractions increasing with temperature. Compared to the other equilibrium calculations the temperature interval is shortened to more reasonable temperatures which the CFB boiler do operate at. The equilibrium however is not affecting the concentrations within these temperatures significantly when these inlet fractions were chosen. It can therefore be concluded that the KOH fraction in the reactor is the K fraction minus the Cl and two times the S fraction. The chlorine species that are not KCl are always HCl, as shown in Figure 4.9.

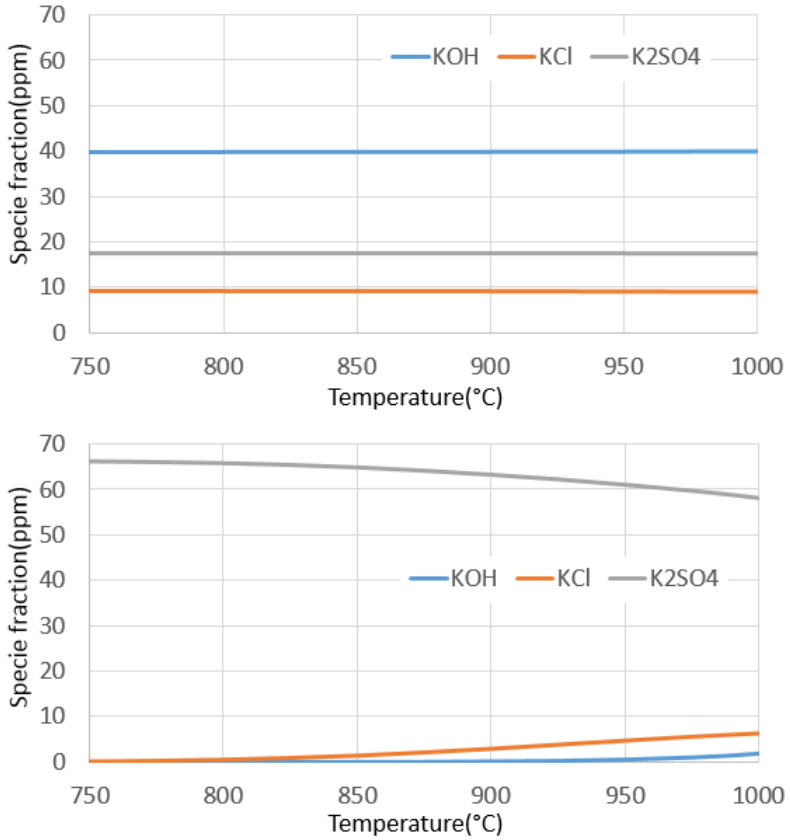

Figure 4.23: Equilibrium fractions for KCl, KOH and K_2SO_4 vs temperature for the cases with and without sulfur feeding. The plot is adjusted for K_2SO_4 so that each mole of K_2SO_4 is shown as 2 moles since it hold two K molecules. Blue is KOH, red is KCl and grey is K_2SO_4. The inlet fraction of Cl is 8.4ppm, S is both 8.9 and 34ppm while K is 67 ppm.

4.3.3 Model representation of the experiments

A model was created with the amount of sulfur detected before the sulfur feeding and during the sulfur feeding. Since there were uncertainties about the alkali content in the biomass and that KOH fraction showed to be crucial for CO oxidation, KOH was varied and it was assumed that no KCl and no HCl was present. It was calculated from the data evaluation that there would be about 67 ppm of potassium species

and 8.9 ppm of chlorine species at the inlet. Assuming all Cl species is released as KCl and that therefore 58 ppm should be present as KOH.

That setup resulted in the plot shown in Figure 4.24, plotting CO concentration at the outlet varying KOH, since KOH showed to be crucial for CO oxidation. The figure shows that both SO_2 concentrations gives a minimum CO outlet at different KOH inlet concentrations. The figure shows that the SO_2 addition gave higher CO outlet concentration at the calculated KOH inlet fraction of 56 ppm. This implies that the model does not represent the experiments well in terms of CO oxidation. In this model, the KOH fraction had to be larger than 150 ppm for the sulfur feeding case to be beneficial in CO oxidation. The CO fraction was around 150 ppm without sulfur feeding, in this model to CO is never above 60 ppm within the plotted range, which makes the model even less representative.

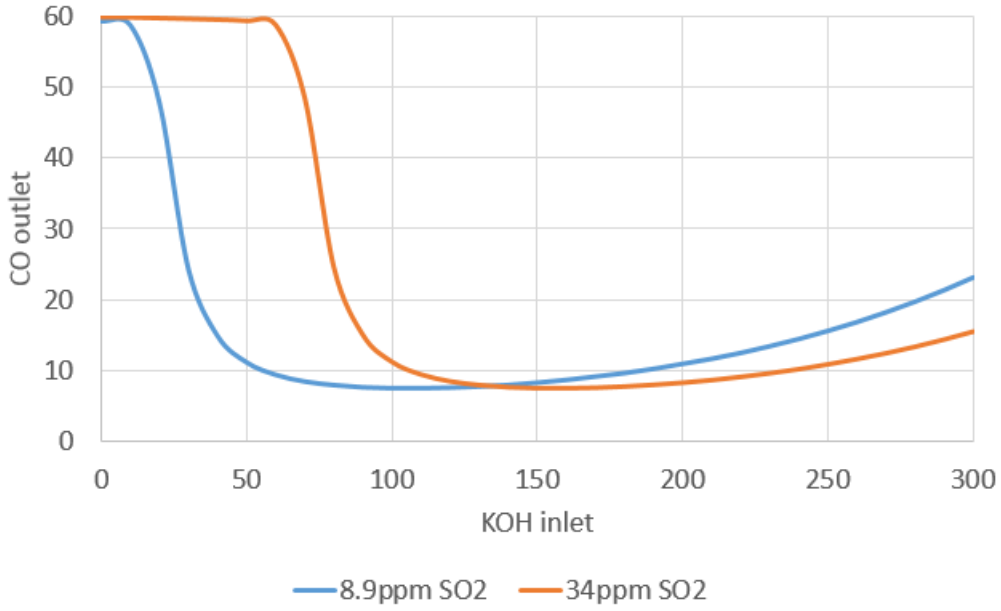

Figure 4.24: CO concentration at the outlet of the PFR reactor vs inlet concentration of KOH. The blue plot represents the case without sulfur addition(SO_{2in} = 8.9ppm) and the red with the sulfur feeding(SO_{2in} = 34ppm). Temperature kept constant at 800°

Investigations were made slightly changing parameters such as KCl, SO_2, CO, inlet, temperature and residence time. However none of these changes created a model where the sulfur feeding case yielded significantly lower CO outlet. However, the previous studies have shown that a large excess of KOH decreases CO oxidation and to create a model where two different SO_2 inlets yields large differences in CO concentration, the SO_2 inlet fraction have to be very different. In that way, the amount of excess KOH is largely different and where the case with low SO_2 inlet gives more KOH excess which is inhibiting CO oxidation. Nevertheless, the fuel report showed that there are no more than 0.084 weight % potassium in the fuel, which according to the calculations gave 65ppm potassium in the boiler. That small amount of potassium can not by itself affect CO oxidation in the way as

the sulfur addition in the experiments did. Therefore it is suggested that there are other conditions in the boiler affecting CO oxidation. The PFR reactor in the modelling may not be representative to the boiler, the boiler might not have perfectly mixed species at the cyclone, even though the cyclone stirs the gas. Only gas phase reactions were included in the modelling whereas the boiler have solids as the fuel and the bed material. However, it is not likely that the flow after the cyclone has much solids since the fuel has vaporized and the bed material is returned to the combustion chamber.

5
Conclusion

This thesis project investigates the influence of the K-S-Cl species on combustion, mainly CO oxidation. By evaluating experiments in a CFB boiler and creating models with similar operating conditions it was found that the K/S/Cl ratio plays an important role in CO oxidation.

Both the experiments and the modelling showed that the K/S/Cl ratio affected CO oxidation. However the effects were larger in terms of CO oxidation compared to K/S/Cl ratio in the experiments than in the models. In order to create models representing the CO oxidation pattern in the experiments, the potassium fraction had to be increased to levels that was not present in the boiler. The models shows that it is mainly KOH in excess that affects CO oxidation. The larger the KOH excess is, the less CO is oxidised. By reducing the residence time in the reactor, the effects are even larger. The models also show that KOH excess have two reaction mechanisms affecting CO oxidation. There are one reaction improving CO oxidation and one mechanism inhibiting CO oxidation. With small excess of KOH the effect of the improving mechanism are larger than the inhibiting, but as the larger the KOH excess grows, the more the inhibiting mechanism takes over.

During the project it was discovered that favourable conditions for CO oxidation are large temperatures, large residence times and low KOH excess. The equilibrium calculations shows that potassium is most likely to form K_2SO_4, then KCl and then KOH if there are enough with other species forming these molecules. That suggests that adding sulfur makes KCl and KOH forms K_2SO_4, improving CO oxidation. Since that was made and obtained in the experiments, it was concluded that the added sulfur formed K_2SO_4, giving less KOH excess which improved CO oxidation in the experiments. Continuous sulfur feeding in the CFB boiler moved the overall combustion more to the bottom of the bed and less in the cyclone. That was most probably since the added sulfur decreased the excess KOH in the bottom of the bed, improving CO oxidation in that region which led to that less CO was available in the cyclone to oxidise. However, in H12 CO was decreased but not fully oxidized, meaning that the last oxidation must have happened in or after the cyclone.

Chlorine is mainly present as KCl and has less improving effect on CO oxidation. KCl is only sulfated when there are no more KOH excess and an excess of KCl inhibits CO oxidation. However, sulfur additions decreases KCl content since K_2SO_4 and HCl are formed, reducing corrosive substances in the boiler which might be of greater importance than improving CO oxidation.

A model created to compare with the experiments gives a case where the CO oxidation was higher when sulfur was added, in contrast to the experiments. Similar models, changing parameters slightly gives no result with lower CO oxidation when sulfur was added. It may therefore be other conditions in the boiler that is affected by sulfur injections affecting CO oxidation. This, however, was not investigated in this project.

The overall conclusion that low KOH excess yields improved CO oxidation and that addition of sulfur makes K_2SO_4 form from KOH provides the suggestion that adding sulfur will decrease CO concentration. However, the closer the system is to have stoichiometric amount of sulfur to potassium, the more likely it is to have SO_2 in the outlet due to bad mixing or adding excess of sulfur. Therefore the suggested sulfur adding unit must be well developed in order not to create SO_2 in the outlet. Judging the sulfur additions from the top of the cyclone and the equilibrium calculations, K_2SO_4 will form directly when KOH is in contact with SO_2 at temperatures around 800 °C making it not a kinetics issue for SO_2 to form K_2SO_4 than a mixing issue.

6
Future work

This project has discovered interesting patterns of how alkali metals and sulfur influence oxidation of CO, which should be further investigated. The modelling results needs to be compared with real experiments in order to increase validity. These experiments should be executed with environments as similar as possible as in the modelling and then compared. Since the models did not represent the experiments in the CFB boiler well, the results from the experiments should also be compared with the CFB experiments.

6.1 Setup of experiments

The new experiments should be made on a lab scale with a tube representing a PFR reactor. The study of residence time and temperature dependency showed that they were crucial to how much CO would oxidize, leading to that these parameters have to be well controlled. The residence time can be controlled by the inflow and the temperature can be controlled by an external heat source. The gas mixture should again represent the flue gas after the cyclone where the main components should be N_2, H_2O, CO_2, O_2, H_2 and CO. These species can be added from gas bottles for each specie. However, the interesting specie that also should be injected is KOH since that was the specie that affected CO oxidation most. KOH can be solved in water and that solution can then be sprayed to the gas inlet mixture. nevertheless, the potassium will be present as a cation in the water solution and hopefully forms KOH at the very inlet of the reactor. That may however affect the whole combustion chemistry and it is crucial to get this operation to work well. The interphase chemistry of vaporisation of potassium should therefore also be investigated if this addition method is used. Sulfur can be added, as in the CFB experiments, by elementary sulfur and assume that everything oxidises to SO_2 instantaneously by Reactions 2.9 and 2.10, as has been made in this project.

6.2 Experiments

Due to possible losses such as bad mixing or stagnant zones in the reactor, tests without K/S/Cl should be performed where CO outlet concentration should be measured. At residence time of 0.64 s and temperature of 790 °C, the CO outlet concentration was about 110 ppm, whereas for 800 °C the temperature was about 60ppm. This will provide a base case that can be compared when K-S-Cl species are introduced.

One study should be made to examine if sulfur and potassium interacts and form K_2SO_4. The modelling always resulted in that all possible K_2SO_4 was formed, meaning that if the amount of potassium is inserted to twice the amount of sulfur, all sulfur and potassium should form K_2SO_4. The CO concentration in the outlet for this experiment should be compared with a case without adding KOH. If all KOH forms K_2SO_4 the CO outlet concentration should be the about same for both tests, as Figure 4.10.

Other experiments can be made investigating the influence of KOH without the presence of Cl and S. The modelling showed that small KOH inlets improved CO oxidation while large inlets decreased CO oxidation. The CFB experiments however showed that less KOH excess, which probably was achieved when the added sulfur formed K_2SO_4, only improved CO oxidation. Many cases would be made in order to get as close KOH inlet interval as possible making it easier to identify trends from the plotting.

The influence of chlorine is also crucial to study. Addition of KCl together with sulfur should be compared with addition of KOH with the same sulfur content. Since the equilibrium showed that chlorine was most likely to be present as KCl, no other chlorine species needs to be added. According to the equilibrium and the models, all KCl should form K_2SO_4 if there is enough sulfur. The studies can be further performed by injecting the same amount of potassium in each experiment, but change the KOH/KCl ratio. According to Figure 4.20 the more KCl the case has, when sulfur also is added in excess, the higher the CO concentration should be.

Since K_2SO_4 and KCl will stick to the surface inside the reactor, the ash content in the reactor can be measured. A specie that has been left out of this project is K_2CO_3, which also can be formed. How well the assumption of ignoring K_2CO_3 and other potassium species was could be examined by measuring its existence in the ashes. To be able to measure that, a small piece of metal should be inserted in the reactor, absorbing ashes. With this method it can be seen if all injected KCl forms K_2SO_4 or if some KCl can be found as ashes.

Bibliography

[1] Dell'Antonia D. (2013) Biomass Combustion. Publication. University of Udine

[2] Birol F. (2016) Key world energy statistics. Publication. International Energy Agency

[3] Ekvall T. (2014). High-Temperature Corrosion Chemistry in Oxy-Fuel Combustion. PhD Thesis. Chalmers University of Technology. Department of Energy and Environment.

[4] Jenkins B.M., Baxter L-L et al. (1998). Combustion properties of biomass. Technical report. Department of Biological and Agricultural Engineering, University of California, Davis, CA, USA. http://dx.doi.org/10.1016/S0378-3820(97)00059-3.

[5] Li B., et al. (2013). Post-flame gas-phase sulfation of potassium chloride. Article. Combustion and Flame http://dx.doi.org/10.1016/j.combustflame.2013.01.010.

[6] Hindiyarti L., et al. (2007). An exploatory study of alkali sulfate aerosol formation during biomass combustion. Article. Fuel First. http://dx.doi:10.1016/j.fuel.2007.09.001.

[7] Wang L., et al. (2012). A critical review on additives to reduce ash related operation problems in biomass combustion applications. Technical report. Norwegian University of Science and Technology, Trondheim, Norway. http://dx.doi:10.1016/j.egypro.2012.03.004.

[8] Kassman H., N. F., Å. L-E. (2013). The effect of oxygen and volatile combustibles on the sulphation of gaseous KCl. Article. Combustion and Flame. http://dx.doi.org/10.1016/j.combustflame.2013.04.018.

[9] Kassman H. (2012). Strategies to reduce gaseous KCl and chlorine in deposits during combustion of biomass in fluidized bed boilers. PhD Thesis. Chalmers University of Technology.

[10] Wang L., Lovas T., Houshfar E. (2014). Effect of sewage sluge addition on potassium releas and ash transformation during wheat straw combustion. Technical report. Norwegian University of Science and Technology, Trondheim, Norway.

[11] Kondratiev V.N., Azatyan V.V., (1973). HO_2 radicals in combustion reactions. Technical report. The academy of science of the S.S.S.R.

[12] Baldwin R.R, et al., (1970) The carbon monoxide-sensitized decomposition of hydrogen peroxide. Technical report. University of Hull.

[13] Glarborg P., et al. (1996). Impact of SO_2 and NO on CO oxidation under post-flame conditions. Techical report. Technical University of Denmark.

[14] Marinkovic J., et al. (2015). Characteristics of olivine as a bed material in an indirect biomass gasifier. Technical report. Chalmers University of Technology.

A

Appendix 1

In this appendix, reactions rates which have been discussed in the report, assumptions, additional models and calculations are shown. These are not necessary for the report but provide evidence on why certain choices and assumptions have been made.

A.1 Integrated reactions rates

In this section, integrated reaction rates that have been discussed in the report are shown. These numbers should only be considered by comparing to each other, examining which reactions are dominant.

A.1.1 The study varying SO_2 in section 4.2.2

In table A.1 the integrated reaction rates forming K_2SO_4 from KOH is presented when KOH is in large excess(2S/K=0.5). Reaction 2.13 is much higher since it is involved in the excess KOH reactions throughout the whole reactor. However it is seen that when KSO_4 is formed, the last steps aer split into one main path with reaction 2.25 and 2.26 and one minor with reaction 2.27.

Table A.1: Table of integrated reaction rates(kmol/m^3) including KOH for the cases with different 2S/K ratios.

Reaction	Reaction rate
2.13	-28.141
2.23	0.576
2.24	0.576
2.25	0.531
2.27	0.041
2.26	0.533

In table A.2, the integrated reaction rates of KOH containing reactions is presented for the study where the influence of different 2S/K ratios were investigated. That study operated at 790°C, normal residence time and without chlorine species.

Table A.2: Table of integrated reaction rates(kmol/m^3) including KOH for the cases with different 2S/K ratios.

Reaction	**2S/K 0.57**	**2S/K 0.7**	**2S/K 0.83**
2.15	14.346	9.950	4.888
2.14	41.182	35.342	24.758
2.16	-4.709	-3.721	-2.359
2.13	-51.992	-43.015	-28.962
2.17	-0.821	-1.057	-1.284
2.26	-0.836	-1.049	-1.2638
Total	-2.769	-3.461	-4.150

In table A.3, the integrated reaction rates of KO containing reactions for the same study as above. Only the significant reactions are included in the table.

Table A.3: Table of integrated reaction rates(kmol/m^3) including KOH for the cases with different 2S/K ratios.

Reaction	**2S/K 0.57**	**2S/K 0.7**	**2S/K 0.83**
2.18	0.837	0.507	0.223
2.16	4.709	3.721	2.359
2.32	0.768	0.371	0.152
2.31	-6.299	-4.619	-2.7835
Total	0.0006	-0.003	0.0008

In table A.4, the integrated reaction rates of OH containing reactions for the same study as above. Only the 8 largest reactions are included in the table. Many more reactions with OH occur which is not mentioned here.

Table A.4: Table of integrated reaction rates(kmol/m^3) including OH reaction for the cases with different 2S/K ratios.

Reaction mechanism	**2S/K 0.57**	**2S/K 0.7**	**2S/K 0.83**
2.3	25.876	30.755	33.912
2.5	7.267	6.449	5.476
2.6	100.391	91.401	77.717
2.7	26.492	36.823	51.591
2.8	17.599	29.051	50.034
2.29	-91.836	-94.236	-97.297
2.8	-12.560	-20.733	-35.708
2.28	-37.116	-38.4276	-39.7167
Total	-0.001	0.042	0.003

A.1.2 Reactions path for KCl to K_2SO_4

A model with only KCl as K specie was made to examine the paths from KCl to K_2SO_4. Table A.5 shows how K_2SO_4 was formed. It shows that the path for KCl to K_2SO_4 mainly takes the reaction path through formation of K, then into KSO_2 and KSO_4. About 80 % of the KSO_4 forms $KHSO_4$ and then K_2SO_4 whereas 20% of the KSO_4 forms K_2SO_4 directly.

Table A.5: Table of integrated reaction rates(kmol/m^3) including OH reaction for the cases with different 2S/K ratios.

Reaction	Share of K_2SO_4 formation(%)
A.1	79.3
A.2	18.2
2.26	2.3

$$KHSO_4 + KCl \longrightarrow K_2SO_4 + HCl \tag{A.1}$$

$$KSO_4 + KCl \longrightarrow K_2SO_4 + Cl \tag{A.2}$$

A.1.3 Reactions of only sulfur

In Figure A.1 the reaction path of SO_2 to S is shown. This is the path in which 99% of all S reacts. About 66% forms SO_2 by Reaction A.5 and 33% forms SO_2 by Reaction A.4. This proves that SO_2 is a good assumption to have as an inlet.

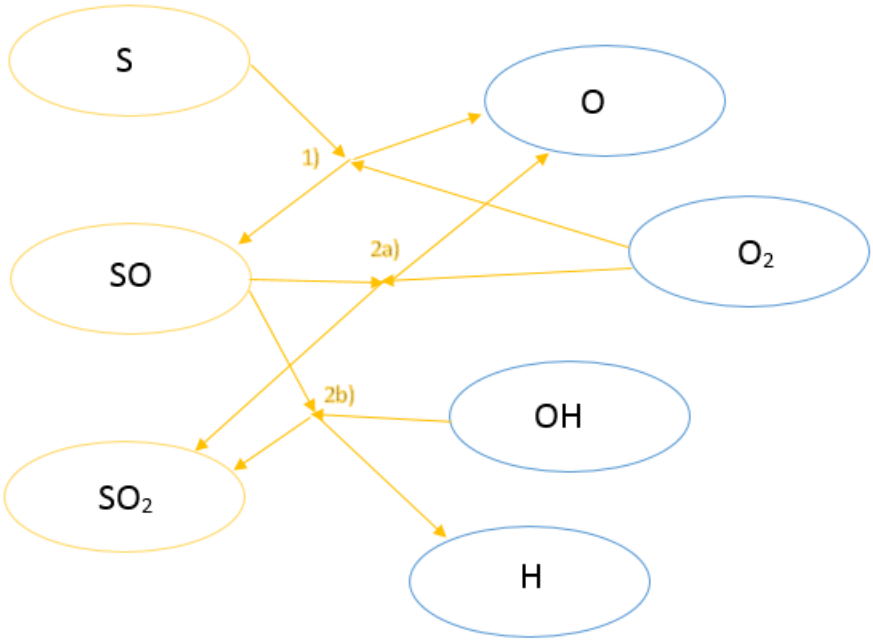

Figure A.1: Reaction path for S to SO_2. This model had 100ppm of S as inlet, no chlorine and no potassium. Reaction 1) is Reaction A.3, 2a) is A.4 and 2b) is A.5.

$$S + O_2 \longrightarrow SO + O \tag{A.3}$$

$$SO + OH \longrightarrow SO_2 + H \tag{A.4}$$

$$SO + O_2 \longrightarrow SO_2 + O \tag{A.5}$$

A.2 Additional models

This section in the appendix shows how other parameter choices affect CO oxidation.

A.2.1 Residence time and temperature plots

To show how only changing residence time or temperature affected the whole CO oxidation, more figures will be shown. In Figure A.2, the influence of decreasing residence times are shown. It shows that lower residence times yields higher CO concentration, especially in region III.

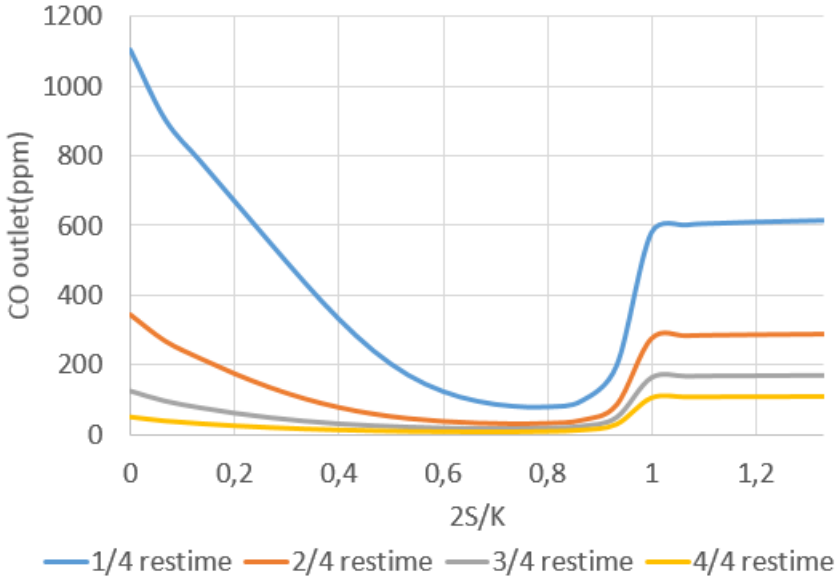

Figure A.2: CO outlet concentration vs 2S/K inlets for different residence times compared to the main residence time of 0.64s used.

In Figure A.3, the influence of increasing residence time is shown. Higher residence time yields lower CO concentration, especially in region I.

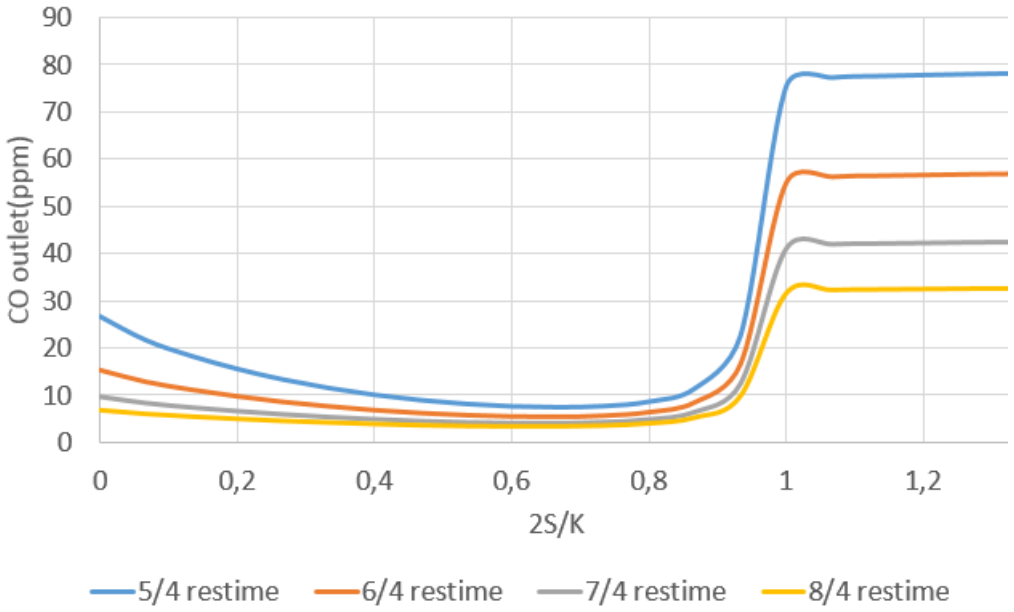

Figure A.3: CO outlet concentration vs 2S/K inlets for different residence times compared to the main residence time of 0.64s used.

In Figure A.4, the influence of higher temperatures on CO oxidation is shown. Already at 820°C the CO level is greatly reduced. The figure does not show it that well, but at 850°C the CO outlet concentration is between 0.5 and 1.5 ppm whereas at 880°C the CO outlet concentration is lower than 0.2 ppm. Thus, the 2S/K ratio has no effect on systems with residence time of 0.64 and temperatures above 850°C.

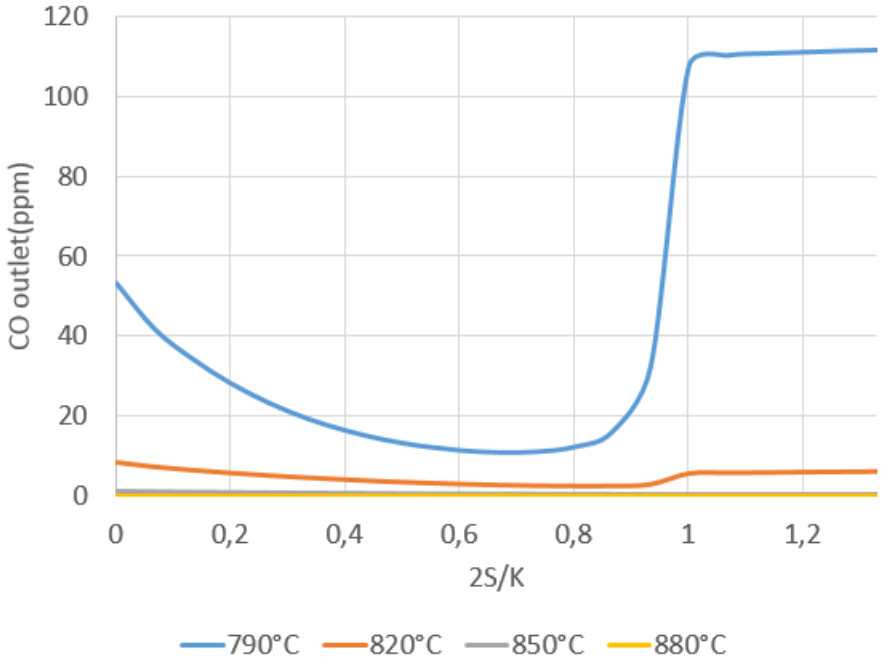

Figure A.4: CO outlet concentration vs 2S/K inlets for different temperatures.

In Figure A.5 the influence of lower temperatures on CO oxidation is shown. A lower

temperature yields higher CO concentration. At 700° region III has an interesting different pattern as 2S/K is increased. This is however not further analyzed.

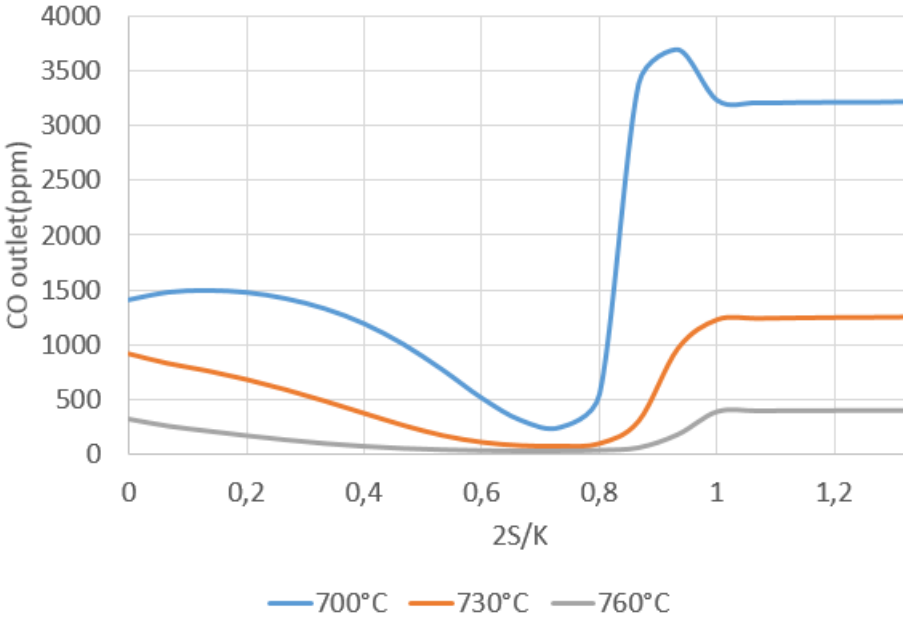

Figure A.5: CO outlet concentration vs 2S/K inlets for different temperatures.

A.2.2 Influence of more KCl than KOH

Figure A.6 shows CO outlet against 2S/K inlet. Since the report only shows cases with more KOH than KCl, this plot shows how the CO outlet is affected by higher KCl ratio, even though the total K content is constant at 300ppm. This figure also shows when only KCl is the potassium specie at the inlet. That case has always higher CO outlet than the other cases at the same 2S/K ratio. This figure only amplifies the statement in the report, which were that KCl do not improve CO oxidation by sulfur addition.

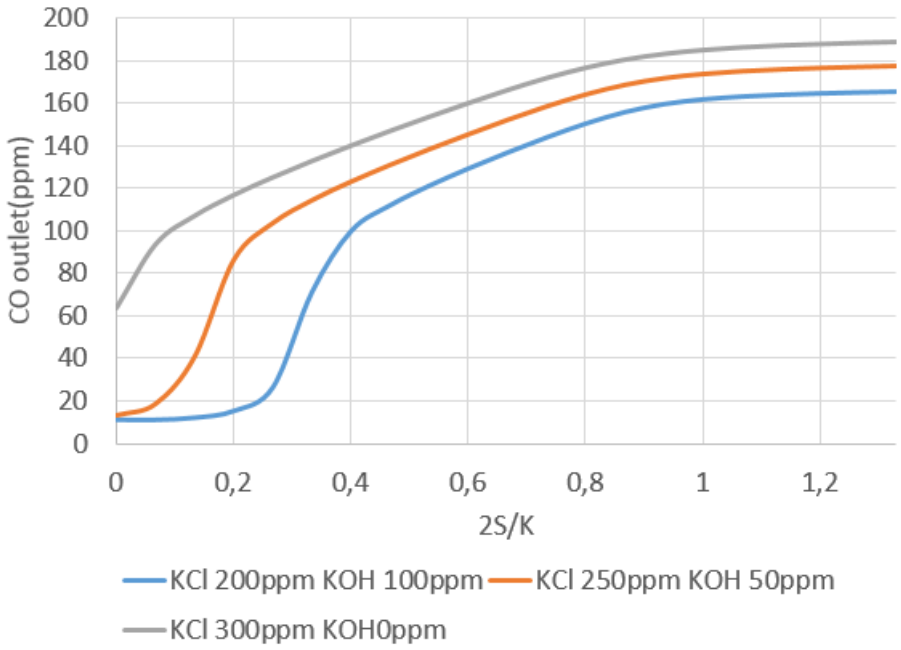

Figure A.6: CO outlet concentration vs 2S/K inlets for different amounts of KCl and KOH, where total K content is 300ppm.

A.2.3 Sulfur equilibrium without K and Cl

Figure A.7 shows an equilibrium case were S is added to the main flow with no K or Cl species. The figure shows that almost all sulfur is present as SO_2, some SO_3 at colder temperatures and no S. This figure shows that it was reasonable to add sulfur as SO_2 instead of S in the modelling.

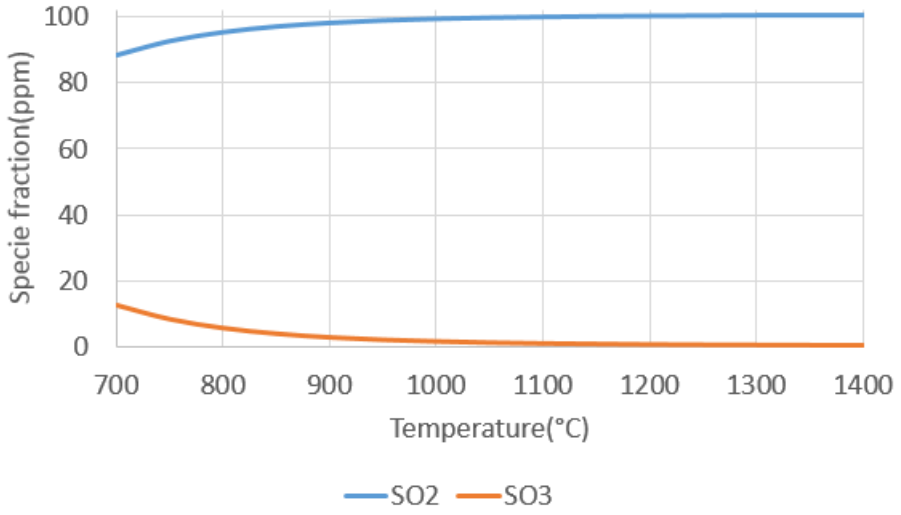

Figure A.7: Equilibrium calculation of sulfur species. S was added with 100ppm to the main flow without K or Cl species.

A.3 Heat balance in the CFB boiler

The heat balances was executed according to equation A.6. C_p values were calculated by equation A.7 for each main specie, mass flow taken from the fuel and air flow inlet and temperature difference taken by average values where the temperature seems to be stable. $dQ_{bottombed}$ = 102.5*38.72*6.86 = 27.23kW. $dQ_{cyclone}$ = 102.5*38.25*-5.18 = -20.3kW.

$$Q = \dot{n} C_p \Delta T \tag{A.6}$$

$$C_{p,i} = A_i + B_i T + C_i T^2 + D_i T^3 \tag{A.7}$$